JGR Earth Surface

RESEARCH ARTICLE
10.1029/2021JF006135

Pleistocene Megaflood Discharge in Grand Coulee, Channeled Scabland, USA

K. E. Lehnigk[1] and **I. J. Larsen**[1]

[1]Department of Geosciences, University of Massachusetts Amherst, Amherst, MA, USA

Key Points:

- Grand Coulee, the largest canyon in the Channeled Scabland, was carved by megafloods from the drainage of Pleistocene glacial Lake Missoula
- Geologic evidence and hydraulic models indicate ~2.6 million $m^3\ s^{-1}$ discharges when upper Grand Coulee incised by headward waterfall retreat
- Waterfall retreat can form large bedrock canyons with smaller discharge than required to inundate present-day topography to high-water marks

Supporting Information:

Supporting Information may be found in the online version of this article.

Correspondence to:

K. E. Lehnigk,
klehnigk@umass.edu

Citation:

Lehnigk, K. E., & Larsen, I. J. (2022). Pleistocene megaflood discharge in Grand Coulee, Channeled Scabland, USA. *Journal of Geophysical Research: Earth Surface*, *127*, e2021JF006135. https://doi.org/10.1029/2021JF006135

Received 19 FEB 2021
Accepted 21 DEC 2021

Author Contributions:

Conceptualization: K. E. Lehnigk, I. J. Larsen
Data curation: K. E. Lehnigk, I. J. Larsen
Formal analysis: K. E. Lehnigk, I. J. Larsen
Funding acquisition: I. J. Larsen
Investigation: K. E. Lehnigk, I. J. Larsen
Methodology: K. E. Lehnigk, I. J. Larsen
Project Administration: I. J. Larsen
Resources: I. J. Larsen
Supervision: I. J. Larsen
Validation: K. E. Lehnigk, I. J. Larsen
Visualization: K. E. Lehnigk, I. J. Larsen
Writing – original draft: K. E. Lehnigk, I. J. Larsen
Writing – review & editing: K. E. Lehnigk, I. J. Larsen

Abstract Bedrock erosion and canyon formation during extreme floods have dramatically altered landscapes on Earth and Mars. Grand Coulee was carved by outburst floods from Pleistocene glacial Lake Missoula and is the largest canyon in the Channeled Scabland, a megaflood-scoured landscape in the northwestern USA. Quantifying paleo-discharge is required to understand how landscapes evolve in response to extreme events, but there are few constraints on the magnitude of the floods that incised Grand Coulee; hence, we used hydraulic modeling and geologic evidence to quantify paleo-flood discharges during different phases of canyon incision. When upper Grand Coulee was incising by headward waterfall retreat, the paleo-discharge was $2.6 \times 10^6\ m^3\ s^{-1}$, which produced shear stresses great enough to cause the waterfall to retreat via toppling of basalt columns. The largest possible flood through upper Grand Coulee, a Missoula flood which raised glacial Lake Columbia to a stage of 750 m, produced a modeled discharge of $7.6 \times 10^6\ m^3\ s^{-1}$. The discharges associated with waterfall retreat and drainage of glacial Lake Columbia are >80% and ~50% lower, respectively, than the $14–17 \times 10^6\ m^3\ s^{-1}$ discharge predicted by assuming the present-day topography was inundated to the elevation of high-water marks. Due to bedrock incision, high-water marks may overestimate paleo-flow depth in canyons carved by floods, hence bedrock erosion should be considered when estimating paleo-discharge in flood-carved canyons. Our results indicate that outburst floods with discharges and flow depths much lower than those required to inundate high-water marks are capable of carving deep canyons.

Plain Language Summary The Channeled Scabland of eastern Washington, USA contains huge canyons carved by ice-age megafloods. However, uncertainty regarding the feedbacks between flooding and erosion makes it difficult to constrain the size of the floods that carved these canyons. High-water evidence is often used to constrain the depth and discharge of outburst floods by assuming canyons were filled with water. We used numerical models to simulate discharge through Grand Coulee, the largest canyon in the Channeled Scabland, where geological evidence indicates a waterfall—many times larger than Niagara Falls—migrated up the canyon. The flood discharge required to inundate high-water marks when the waterfall was retreating was approximately 15%–20% of the discharge that reaches the high-water marks in the present-day topography. The largest possible flood through the canyon, which was modeled from upstream lake stages, does not inundate high-water marks, indicating the present-day canyon was never filled with water. Instead, the high-water marks were emplaced by smaller floods prior to the deepening of the canyon by waterfall erosion. These findings suggest paleo-flood discharge can be over-estimated in canyons that formed by waterfall retreat if erosion is not taken into account.

1. Introduction

Many landscapes on Earth contain evidence of extreme floods triggered by the failure of glacial and other natural dams or by release of water from subglacial lakes (Baker, 1973, 2002, 2008; Baynes, Attal, Dugmore, et al., 2015; Bretz, 1923; Carling, 1996; Gupta et al., 2007; Lamb et al., 2008, 2014; Lapotre et al., 2016; Lewis et al., 2006; Malde, 1968; Montgomery et al., 2004; O'Connor, 1993). Ancient channels, much larger than those on Earth, provide evidence of extensive flooding on the surface of Mars (Baker, 1982; Baker & Milton, 1974; Sharp & Malin, 1975). Quantifying the discharges and shear stresses produced by outburst floods is important for understanding the role that rare, extreme floods play in eroding landscapes and shaping planetary surfaces (Baker, 1973, 1979; Baynes, Attal, Dugmore, et al., 2015; Cook et al., 2018; Denlinger & O'Connell, 2010; Garcia-Castellanos & O'Connor, 2018; Goudge & Fassett, 2018; Lamb & Fonstad, 2010; Lamb et al., 2008; Lang et al., 2013; Larsen & Lamb, 2016; Larsen & Montgomery, 2012; O'Connor & Baker, 1992; Turzewski et al., 2019). Delivery of freshwater to oceans by large floods has been linked to deglacial climate change; for example, flooding from glacial lakes of the waning Laurentide Ice Sheet is thought to have triggered abrupt climate change via alteration

of thermohaline circulation (e.g., Barber et al., 1999; Clark et al., 2001), and delivery of glacial meltwater to the Pacific Ocean by the Missoula floods is thought to have contributed to global cooling (Praetorius et al., 2020). Determining the discharges and volumes of freshwater delivered to oceans by floods is important for assessing whether terrestrial meltwater sources alone are sufficient for triggering abrupt global cooling, or alternatively, whether melting large volumes of sea ice is required (Condron et al., 2020). Quantifying flood discharge through the Mars Outflow Channels also has paleoclimate implications, as the transfer of floodwaters to a northern ocean would have dramatically altered the Martian atmosphere (e.g., Baker et al., 1991).

Total water volumes are difficult to constrain for floods from subglacial lakes (Baynes, Attal, Niedermann, et al., 2015) and Martian aquifers (Carr, 1979). Lake shorelines can provide constraints on the maximum water volume available for a single flood, but where field evidence indicates there were multiple floods (e.g., Atwater, 1986; Waitt, 1985), it is difficult to link downstream evidence of flooding with specific lake levels. In such cases, the lack of information on the integrated discharge from multiple floods makes it difficult to link flood magnitude with erosion and landscape evolution. Where lake volume information is lacking or where floods diverged into multiple channels, the sizes of channels and mobilized sediment provide some of the only evidence that can be used to reconstruct discharge in individual flow paths (Baker, 1973; Larsen & Lamb, 2016; Lapotre et al., 2016; Lewis et al., 2006). Even where lake volumes can be constrained, discharge estimates are required to constrain dam failure mechanisms (O'Connor & Baker, 1992), to estimate erosion and sediment transport thresholds (Baker, 1973; Lamb & Fonstad, 2010), and to predict the extent of flood inundation (Denlinger & O'Connell, 2010; Turzewski et al., 2019). However, constraining paleo-discharge in canyons carved in their entirety by floods is challenging, because topography and flow hydraulics co-evolve (Lamb & Fonstad, 2010; Lapotre et al., 2016; Larsen & Lamb, 2016). For example, the ability to reconstruct the discharges of catastrophic floods from glacial lakes of the Laurentide Ice Sheet is limited because the spillways, which are carved into unconsolidated glacial till, show evidence of incision during floods that hinders reconstruction of the paleo-flow depth (Kehew, 1982). Similarly, in bedrock canyons carved entirely by floods, the coupled decline in the elevation of the canyon floor and flood stage limits the ability to reconstruct discharge from high-water marks and the post-flood topography (Lamb & Fonstad, 2010; Larsen & Lamb, 2016). Even where floods inundated pre-existing canyons or valleys, the unconstrained magnitude of flood-induced erosion adds an unquantified degree of uncertainty to paleo-discharge estimates (Bretz, 1969). Where changes in topography can be constrained, flood simulations on pre- and post-flood topography can be used to assess the influence of erosion on flood hydraulics (Benito & Thorndycraft, 2020; Lamb & Fonstad, 2010; Larsen & Lamb, 2016).

Here, we reconstruct paleo-flood discharge for upper Grand Coulee, part of the largest canyon complex in the Channeled Scabland, eastern Washington, USA (Bretz, 1932), which has geomorphic characteristics comparable to channels on Mars (Baker & Milton, 1974). We use numerical modeling and field evidence to determine the discharges at key times during the history of Grand Coulee's formation, including when the canyon was being incised via headward waterfall retreat. Our work builds on the descriptive model for the evolution of Grand Coulee proposed by Bretz (1932) by placing quantitative constraints on Pleistocene flood discharge, which enhances our ability to link flood discharge, bedrock erosion, and canyon morphology.

2. Study Site

The Channeled Scabland (Figure 1) is a landscape of scoured bedrock, giant current ripples, huge boulder bars, dry waterfalls, streamlined loess hills, and large channels, some which are deeply incised bedrock canyons (Bretz, 1923, 1969; Baker, 1973, 2009; O'Connor et al., 2020). The Channeled Scabland was carved into the Miocene-age Columbia River basalt (Barry et al., 2013) by outburst floods from glacial Lake Missoula (Bretz, 1969; Bretz et al., 1956; Pardee, 1942). Glacial Lake Missoula was a glacial lake in eastern Montana that formed when advance of the Purcell Trench Lobe of the Cordilleran Ice Sheet blocked the Clark Fork River, a tributary to the Columbia River (Pardee, 1942). Failure of the ice dam, by flotation (O'Connor & Baker, 1992) or subglacial tunneling (Clarke et al., 1984), during the late Pleistocene released up to 2,500 km^3 of water into the Columbia River drainage and the Channeled Scabland (O'Connor et al., 2020) (Figure 1a). Sedimentary evidence indicates glacial Lake Missoula drained at least dozens of times during the late Pleistocene (Atwater, 1986; Waitt, 1985) and that the magnitude of the floods varied (Benito & O'Connor, 2003; Smith, 2006).

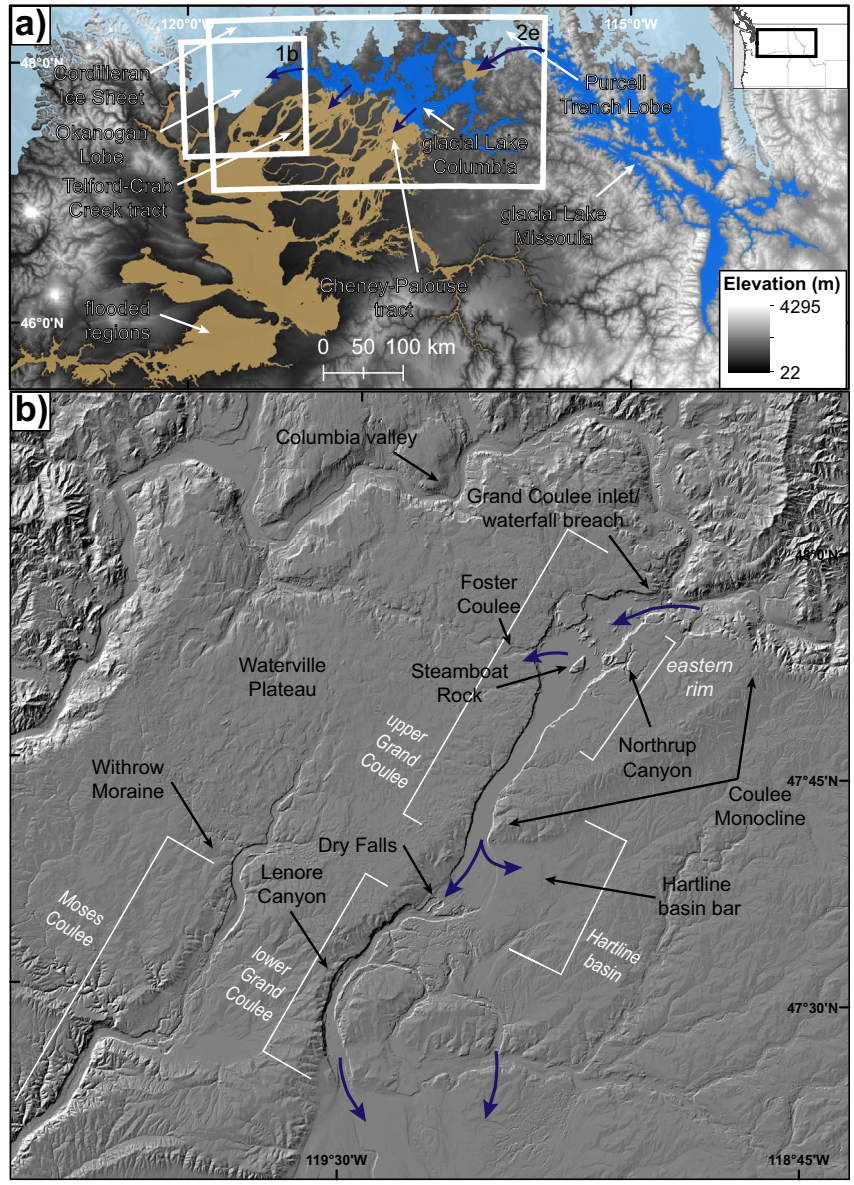

Figure 1. The study area (a) in the northwest USA showing the locations of ice sheets (light blue), glacial lakes (dark blue), and areas inundated by Missoula floods (brown) during the Last Glacial Maximum (Ehlers et al., 2011). (b) Location of Grand Coulee and other geomorphic features in the northwest portion of the Channeled Scabland. Blue arrows show flow directions.

The specific path of the outburst floods varied due to differences in flood size, the changing position of the Okanogan Lobe of the Cordilleran Ice Sheet, and the incision of channels as floodwaters overtopped and spilled out of the valley of the Columbia River and its tributaries across the Columbia Plateau (Bretz, 1969). ^{10}Be exposure dates from flood-transported, iceberg-rafted erratics downstream from the inlet to Grand Coulee are ~18.2 ka, indicating the Columbia valley was not blocked by ice at that time (Balbas et al., 2017). Subsequent advance of the Okanogan Lobe across the Columbia valley impounded flow, forming glacial Lake Columbia (Atwater, 1984; Waitt, 1980). When floods were large or when the Columbia River was blocked, forming glacial Lake Columbia, floods from glacial Lake Missoula spilled south through the Cheney-Palouse and Telford-Crab Creek scabland tracts, and incised Grand Coulee, "the simplest but grandest case of canyon-cutting by glacial streams on the plateau" (Bretz, 1923, p. 632).

Grand Coulee is a system of two canyons, upper and lower Grand Coulee, each of which was incised by headward cataract or waterfall retreat (a cataract is a waterfall with high discharge) driven by the spillover of floodwaters from the Columbia valley (Bretz, 1923, 1932). Floodwaters initially flowed across the low-relief Columbia Plateau until encountering more steeply sloping topography at the Coulee Monocline. A cataract initiated at the monocline, where folding related to regional tectonics had fractured and weakened the basalt (Bretz, 1932). Upper Grand Coulee formed as the cataract retreated upstream via plucking of jointed basalt until it eroded entirely through the drainage divide separating it from the Columbia valley (Bretz, 1923, 1932). After the drainage divide between Grand Coulee and the Columbia valley breached, the floor of Grand Coulee became the lowermost outlet of glacial Lake Columbia, and hence the preferential route for any subsequent floods from glacial Lake Missoula. The incision of upper Grand Coulee generated the longest and deepest canyon in the Channeled Scabland, with a length of 40 km and up to 270 m of relief between the canyon rim and floor; the canyon width is 2–2.8 km in its lower reach and widens to over 8 km upstream. A cataract complex, Dry Falls, separates upper and lower Grand Coulee; lower Grand Coulee developed in a similar fashion via headward cataract retreat (Bretz, 1932).

Steamboat Rock is a basalt monolith in the upstream part of upper Grand Coulee that was preserved when the retreating cataract split and then re-joined upstream, a process similar to that which is creating Goat Island at Niagara Falls (Bretz, 1932). Foster Coulee is located upstream from Steamboat Rock and slopes to the west from Grand Coulee toward the Columbia valley (Figure 1b). If Foster Coulee was carved prior to the retreat of the cataract past Steamboat Rock, it would have been an outlet for some of the floodwater entering Grand Coulee when the Okanogan Lobe blocked the Columbia valley. Northrup Canyon, a second canyon near Steamboat Rock, drains from the eastern rim to the floor of Grand Coulee (Figure 1b). Granitic rock is exposed in Northrup Canyon and in other parts of Grand Coulee upstream from Steamboat Rock where floodwaters incised through the Columbia River basalts (Bretz, 1932); ^{10}Be exposure ages indicate the last floods to incise Northrup Canyon occurred at 15.6 $\pm$ 1.3 ka (Balbas et al., 2017). Glacial erratics, till, and striae on the summit of Steamboat Rock, which is flood-scoured scabland topography, indicate that the Okanogan Lobe advanced into Grand Coulee after the onset of Missoula flooding (Bretz, 1932; Crosby & Carson, 1999). A dark gray diamict exposed near the base of Steamboat Rock has been interpreted to be lodgement till, indicating the Okanogan Lobe advanced into Grand Coulee after the cataract had retreated upstream from Steamboat Rock (Atwater, 1987; Waitt et al., 2021). Glacial striae at the elevation of the canyon floor upstream from Steamboat Rock also support the interpretation that the Okanogan Lobe occupied Grand Coulee after it was incised by floods (O'Connor et al., 2020; Waitt et al., 2021).

If glacial Lake Columbia existed at the time the divide separating upper Grand Coulee and the Columbia valley was breached, a catastrophic flood would have been released through upper Grand Coulee (Bretz, 1969); the flood would have been exceptionally large if the draining of glacial Lake Columbia coincided with a flood from Lake Missoula (Bretz, 1969, p. 527). Blockage of the inlet to upper Grand Coulee by the Okanogan Lobe allowed glacial Lake Columbia to attain stages up to 730 m (O'Connor et al., 2020; Waitt & Thorson, 1983). The elevations of ice-rafted erratics indicate the stage of glacial Lake Columbia increased to 750 m one or more times due to incoming floods from glacial Lake Missoula (Atwater, 1986). A lower, ~470 m-stage glacial Lake Columbia existed after Grand Coulee was incised and the Okanogan Lobe had retreated from upper Grand Coulee, but still blocked the Columbia valley downstream from the coulee inlet (Atwater, 1986; O'Connor et al., 2020; Waitt & Thorson, 1983).

Estimates of the peak discharge for the outflow from glacial Lake Missoula range from ~3×10^6 to 35 $m^3\ s^{-1}$ (e.g., Baker, 1973; Clarke et al., 1984; Denlinger & O'Connell, 2010; O'Connor & Baker, 1992; O'Connor et al., 2020), but because the flow was then distributed across the Channeled Scabland during some floods, the discharges that drove bedrock incision in individual flood routes were smaller (Baker, 1973). There are few constraints on discharge in Grand Coulee. In upper Grand Coulee, one-dimensional step backwater calculations based on high-water marks and the present-day topography indicate the canyon conveyed a discharge of 12–14 $\times 10^6$ $m^3\ s^{-1}$, as calculated by Harpel (1996) and referenced by Harpel et al. (2000), Waitt et al. (2000, 2009, 2021), and O'Connor et al. (2020). Sedimentological data from graded beds separated by varves have been interpreted as flood beds deposited when glacial Lake Columbia occupied part of upper Grand Coulee after it was incised and suggest the minimum flood discharge was 0.13 $\times 10^6$ $m^3\ s^{-1}$ (Atwater, 1987). Such evidence is attributed to smaller, waning Missoula floods (Atwater, 1987). Mechanistic arguments involving canyon head morphology and plucking thresholds indicate a maximum discharge of 0.65 $\times 10^6$ $m^3\ s^{-1}$ for flow through the two main western alcoves of Dry Falls (Lapotre et al., 2016). The discharge through Lenore Canyon, one of several channels

exiting lower Grand Coulee, has been estimated to be 4.5×10^6 m^3 s^{-1}, based on a paleo-flow depth constrained by high-water marks and the present-day canyon topography (Baker, 1973).

3. Hydraulic Modeling

3.1. Numerical Flood Simulations and Paleo-Discharge Reconstruction

We simulated floods through a series of model domains, which are described below (Figure 2). Each model domain represents a distinct, geologically plausible topographic condition that floods may have encountered during sequential phases of the geomorphic evolution of Grand Coulee. Each domain assumes that the Okanogan Lobe blocks the Columbia valley to the west, which causes floods to flow into Grand Coulee. The simulations include both steady-state discharge models designed to determine the discharge that inundates a particular high-water mark, and non-steady discharge simulations from the dam-break release of water impounded by glacial Lake Columbia. The numerical simulations were used to quantify hydraulic parameters, including the spatial extent of flood inundation, maximum flood stage, and bed shear stress.

Floods were numerically simulated using ANUGA, a two-dimensional, finite-volume hydrodynamic modeling toolkit that solves the shallow water equations (Roberts et al., 2015). ANUGA uses a triangular mesh for computation, constructed from 10 m digital elevation model (DEM) data using a maximum triangle area of 5,000 m^2. The DEM data were from the U.S. Geological Survey, locally adjusted to match pre-erosion conditions specified by our inferred sequential history. We used multibeam survey data to generate elevation data in the area that was formerly occupied by glacial Lake Columbia and is now inundated by Lake Roosevelt upstream from Grand Coulee Dam (Ferrari, 2012). The topography beneath Banks Lake, a reservoir in upper Grand Coulee, was generated by digitizing contours of 1:24,000 scale historical U.S. Geological Survey topographic maps, and the topography in areas of lower Grand Coulee that are now natural lakes was generated from bathymetric contour data. The node locations in the computational mesh were automatically generated by ANUGA; in the retreating cataract scenario, additional points were generated along a breakline to define the cataract brink, ensuring that boundaries between mesh cells, where we extracted shear stress values, coincided with the brink. Grids of flow depth and stage were interpolated from the computational mesh at 30 m cell resolution for model timesteps of interest.

All model scenarios used a spatially uniform Manning's roughness coefficient of 0.065. The value of 0.065 is based on the standard deviation of bedrock channel bed elevation measured in Moses Coulee (Larsen & Lamb, 2016), a canyon adjacent to Grand Coulee with comparable bed topography; use of the same roughness coefficient for Grand Coulee also permits direct comparison with prior results (Larsen & Lamb, 2016). It is difficult to retrospectively assess flow roughness for paleo-floods and there is uncertainty in the roughness value, hence we re-ran a subset of the simulations with a roughness coefficient of 0.04. The value of 0.04 was selected to be comparable to values of 0.03 and 0.05 that Harpel (1996) used for channel and overbank areas, respectively. The simulations assume clear water floods with no suspended sediment. Although such an assumption may be realistic for initial phases of lake overtopping, entrainment of sediment due to erosion of bedrock, fine-grained loess, or lacustrine deposits would increase sediment concentrations. Sediment concentrations for the Missoula floods are not constrained, and likely varied in space and time, so we have not attempted to include these effects, but note that shear stresses may have been higher if sediment concentrations increased fluid density. Features along the domain boundary that were impermeable to flow, such as ice, were incorporated as reflective boundaries, whereas flow exited the domain through Dirichlet boundary segments (Figure 2). A reflective boundary condition across the Columbia valley downstream from the inlet to upper Grand Coulee simulates the blocking of the valley by ice, which forces floodwaters to initially pond and then to flow south through the coulee.

For the steady-state flow simulations, water entered the model domain in the Columbia valley upstream from Grand Coulee. A range of discharges of interest for each scenario was simulated using a stair-step hydrograph and the discharge increment varied depending on the model scenario, such that larger increments were used for larger discharges (Table 1). Each discharge was maintained for a model run time of 150,000 s (41.67 hr), which was sufficient time for flow to reach steady state as indicated by constant stage at multiple points throughout the domain; results were saved every 10,000 s (2.78 hr). The purpose of these simulations is not to simulate a Missoula flood hydrograph, but rather to determine the discharge that inundates specific high-water evidence. In the glacial Lake Columbia draining scenarios, the discharge evolved throughout the model domain following the instantaneous removal (e.g., Denlinger & O'Connell, 2010; Turzewski et al., 2019) of the drainage divide or ice

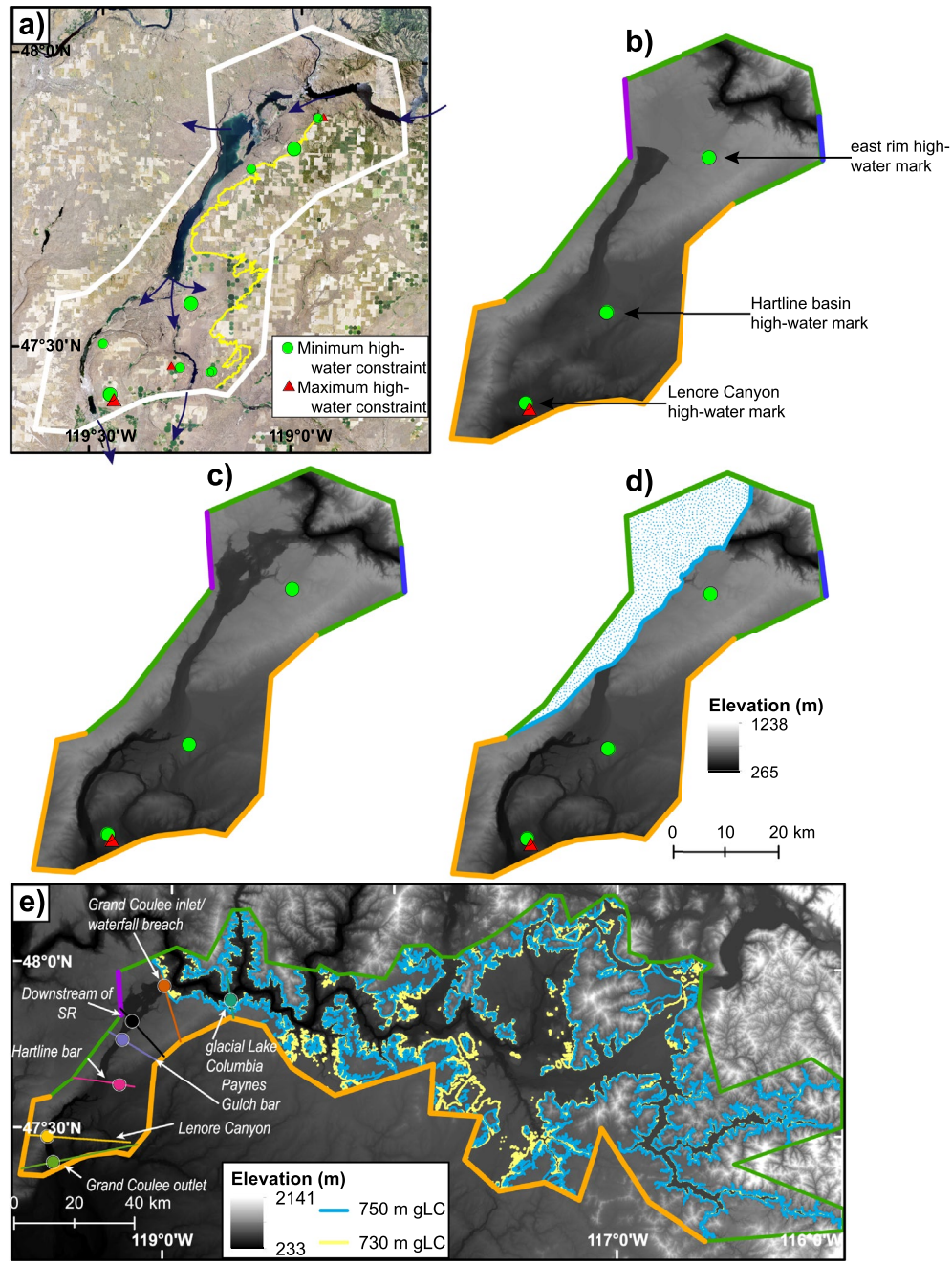

Figure 2. Hydraulic model domains and boundary conditions. (a) The model domain (white polygon) overlying U.S. Department of Agriculture aerial imagery with flood routes shown by blue arrows. High-water evidence is shown by green circles and red triangles; we focus our analysis on the high-water marks shown with the larger symbols. The yellow line shows the approximate high-water limit along the eastern side of the coulee, based on our mapping and that by Bretz (1932). Topography and boundary conditions for (b) the retreating cataract model with a reconstructed cataract in upper Grand Coulee and channel floors in lower Grand Coulee reconstructed between the rims of inner canyons; (c) the present-day topography model; (d) the model representing the time when upper Grand Coulee was filled with ice from the Okanogan Lobe (stippled polygon); and (e) the non-steady dam release models that routed floods from glacial Lake Columbia (gLC) with two initial lake stages at 750 and 730 m. Initial lake extents are shown in blue (750 m initial stage) and yellow (730 m initial stage). Cross-sections and points used to create hydrographs in Figure 6 are indicated as labeled lines and circles. The figure extent in panel (e) corresponds to the white box in Figure 1a. Orange lines indicate open boundaries, green lines indicate closed boundaries, purple lines at Foster Coulee denote a boundary that was either open or closed depending on the model run, and the blue line across the Columbia valley is the discharge inlet.

Table 1
Steady-State Model Runs, Simulated Discharge Ranges, and High-Water-Inundating Discharge Results

Model scenario	Variation	Discharges run, 10^6 m^3 s^{-1} (intervals in parentheses)	Number of discharges run	High-water mark	High-water-inundating discharge, 10^6 m^3 s^{-1}
Reconstructed cataract	Foster Coulee open	1.4–2.7 (0.1)	23	East rim	2.6
		3.0–4.0 (0.5)		Hartline basin	2.4
		5–7 (1)		Lenore Canyon	Min: 1.9 Max: 7.0
		7.5–8 (0.5)			
		9			
	Foster Coulee closed	1.4–2.7 (0.1)	21	East rim	2.6
		3.0–4.0 (0.5)		Hartline basin	1.9
		5.0–5.5 (0.5)		Lenore Canyon	Min: 1.6 Max: 5.0
		6–7 (1)			
Present-day topography	Foster Coulee open	2.6	23	East rim	17
		5–9 (0.5)		Hartline basin	6.5
		10–20 (1)		Lenore Canyon	Min: 5.5 Max: 7.5
		25–30 (5)			
	Foster Coulee closed	4.0–8.0 (0.5)	19	East rim	14
		9–15 (1)		Hartline basin	6.5
		20–30 (5)		Lenore Canyon	Min: 5.5 Max: 7.5
Okanogan Lobe occupying upper Grand Coulee		0.05–0.5 (0.05)	12	East rim	0.45
		0.75–1.0 (0.25)			

dam impounding the lake. No additional discharge (e.g., from a Missoula flood entering the upstream end of the lake) enters the domain; we include potential glacial Lake Missoula inflow via the flood-swollen 750 m glacial Lake Columbia stage. We simulated the first 100,000 s (~27.8 hr) of lake drainage and saved the results every 100 s, which captured the peak discharge. When relevant, hydraulic models for each scenario were run twice; once where flow was allowed to exit the domain via Foster Coulee, and once where Foster Coulee was closed to flow. The two boundary conditions account for different possible configurations of the Okanogan Lobe ice margin. Flow could exit through Foster Coulee toward Moses Coulee when the ice margin was to the north, but when ice advanced across Foster Coulee that flood route was blocked.

We assessed paleo-discharge by determining which of our simulated flows exceeded the elevation of high-water evidence. We used published high-water data (Baker, 1973; O'Connor et al., 2020) from the two locations most relevant for constraining discharge in upper Grand Coulee. In upper Grand Coulee, high-water evidence on the eastern rim constrains the paleo-flood stage (latitude: 47.85010, longitude: 119.00920, and elevation: 744 m; O'Connor et al., 2020). The high-water evidence is a shallow drainage divide which was crossed by floods located near the eastern-most extent of local flooding that separates a loess hill that was isolated from the adjacent loess-covered uplands by flooding. The crossed divide records the minimum flood stage, and hence minimum discharge. We use the elevation of another divide crossed by floods to constrain discharge exiting upper Grand Coulee in Hartline basin, originally reported by Baker (1973), which places a minimum bound on flood stage and discharge (latitude: 47.58210, longitude: 119.25750, and elevation: 552 m; O'Connor et al., 2020). We also show the locations of other high-water evidence in Grand Coulee listed in O'Connor et al. (2020) but focus our interpretations on the locations described above. There are a few other high-water marks on the east rim in upper Grand Coulee, such as stripped basalt (O'Connor et al., 2020), but the divide crossing we use, where loess was eroded without exposing underlying basalt, may place a narrower constraint on the minimum paleo-depth and discharge, as there are only a few meters of elevation difference between the divide crossing and adjacent loess uplands. We also mapped the approximate location of high-water evidence, incorporating earlier mapping by Bretz (1932) as described in the Supporting Information S1, but the maps provide only an approximate limit of flooding, primarily due to the difficulty in determining the extent of flooding in areas where the loess was not extensively eroded.

3.2. Paleo-Discharge During Cataract Retreat

The cataract retreat scenario represents a phase in the evolution of Grand Coulee when the knickpoint that originated at the Coulee Monocline had retreated to the downstream end of Steamboat Rock and before Dry Falls had retreated to its current position (Bretz, 1932). Erosion of gravel deposits led Bretz (1923) to infer that bar deposition in Hartline basin, at the mouth of upper Grand Coulee, occurred prior to erosion at the head of lower Grand Coulee; the gravel deposits were bisected by headward retreat of Dry Falls. Additionally, observations of gravels in Hartline basin indicate the clasts are nearly entirely of basalt composition, suggesting the bar was deposited before the cataract in upper Grand Coulee retreated upstream enough to erode the granitic rock that underlies basalt in the upstream end of the canyon (Bjornstad & Kiver, 2012; Waitt et al., 2021). If the cataract in upper Grand Coulee and the Dry Falls cataract were retreating simultaneously, a similar magnitude flood should inundate both the high-water mark on the east rim and the high-water mark in Hartline basin. The lowest discharge that inundates these two high-water marks therefore places a constraint on the flood magnitude that drove the incision of Grand Coulee via cataract retreat.

We reconstructed the cataract and upstream channel bed topography in upper Grand Coulee by assuming the elevation of the cataract brink was similar to that of the present-day canyon rim (718 m at the upstream-most point). The exact planform shape of the cataract brink at this time is unknown, but we assumed it generally had an amphitheater-shape (e.g., Waitt, 2021). To reconstruct the paleo-channel floor upstream from the cataract, we manually outlined the canyon rims on a 10 m DEM and generated a triangular irregular network (TIN) by interpolating between the points on the canyon rims, converted the TIN to a grid, and merged this grid of the reconstructed cataract topography over the existing, present-day DEM (Figure S1 in Supporting Information S1). The resulting topography is a 192 m-tall backward-facing step in the channel bed (e.g., a cataract or waterfall) with an upstream channel that has a gradient set by the regional slope of the plateau surface at the canyon rim (Figure S1 in Supporting Information S1). In lower Grand Coulee we similarly reconstructed topography by interpolating a TIN across the rims of the inner channels (Jasper Canyon, Lenore Canyon, Spring Coulee, and Dry Coulee), which re-creates a channel floor with an elevation at the present-day brink of Dry Falls (Figure S2 in Supporting Information S1). The interpolated topography was then merged over the topography with the reconstructed cataract in upper Grand Coulee; the topography between Steamboat Rock and the upstream end of Dry Falls was the same as the present-day topography (Figure 2b). It is unlikely that the cataract in upper Grand Coulee retreated to Steamboat Rock with little or no erosion of the inner channels in lower Grand Coulee, which is implied by our topographic reconstruction. However, our primary objective is to simultaneously assess flood inundation in upper Grand Coulee and in Hartline basin without hydraulic influence from Dry Falls, which our topographic reconstruction permits.

The lowest steady-state discharge that inundates the high-water mark on the east rim, which is upstream from the reconstructed cataract, is 2.6×10^6 m^3 s^{-1} when flow is allowed to exit through Foster Coulee (Figure 3) and the same discharge inundates the high-water mark when Foster Coulee is closed to flow (Table 1, Figure S3 in Supporting Information S1). For a scenario with an alternate reconstruction of the paleo-cataract, with an elevation lower than the canyon rim (670 m at the upstream-most point), the discharge required to inundate the high-water mark is somewhat higher (Figures S4–S6 and Table S1 in Supporting Information S1). Similarly, if the high-water mark had been emplaced by an earlier phase of flooding unrelated to cataract retreat and subsequently abandoned, then the discharge we estimate is a maximum value. Simulations using a Manning's roughness coefficient of 0.04 rather than 0.065 predict inundation of the high-water mark on the eastern rim at a minimum discharge of 3.1×10^6 m^3 s^{-1} when flow is allowed to exit through Foster Coulee (Figure S7 in Supporting Information S1). Simulations with the cataract in upper Grand Coulee and the pre-incision topography of lower Grand Coulee reconstructed separately yield similar results (Figures S8–S10 in Supporting Information S1). Hence, the position of the Dry Falls cataract does not affect the flow over the cataract in upper Grand Coulee when it is located at Steamboat Rock. The lowest discharge that crosses the divide at Hartline basin is 2.4×10^6 m^3 s^{-1}, which is consistent with the discharge constrained by the high-water mark on the east rim. While the 2.4×10^6 m^3 s^{-1} discharge inundates the crossed divide, it does not inundate the bar surface to the north. However, a discharge of at least 2.6×10^6 m^3 s^{-1} or a flood from the drainage of glacial Lake Columbia (through the present-day topography) would have inundated that portion of the bar (Figure S11 in Supporting Information S1). Hence, a discharge of approximately 2.6×10^6 m^3 s^{-1} is most consistent with the field evidence and is the maximum plausible flow through upper Grand Coulee prior to headward retreat of the cataract to the drainage divide at the Columbia valley.

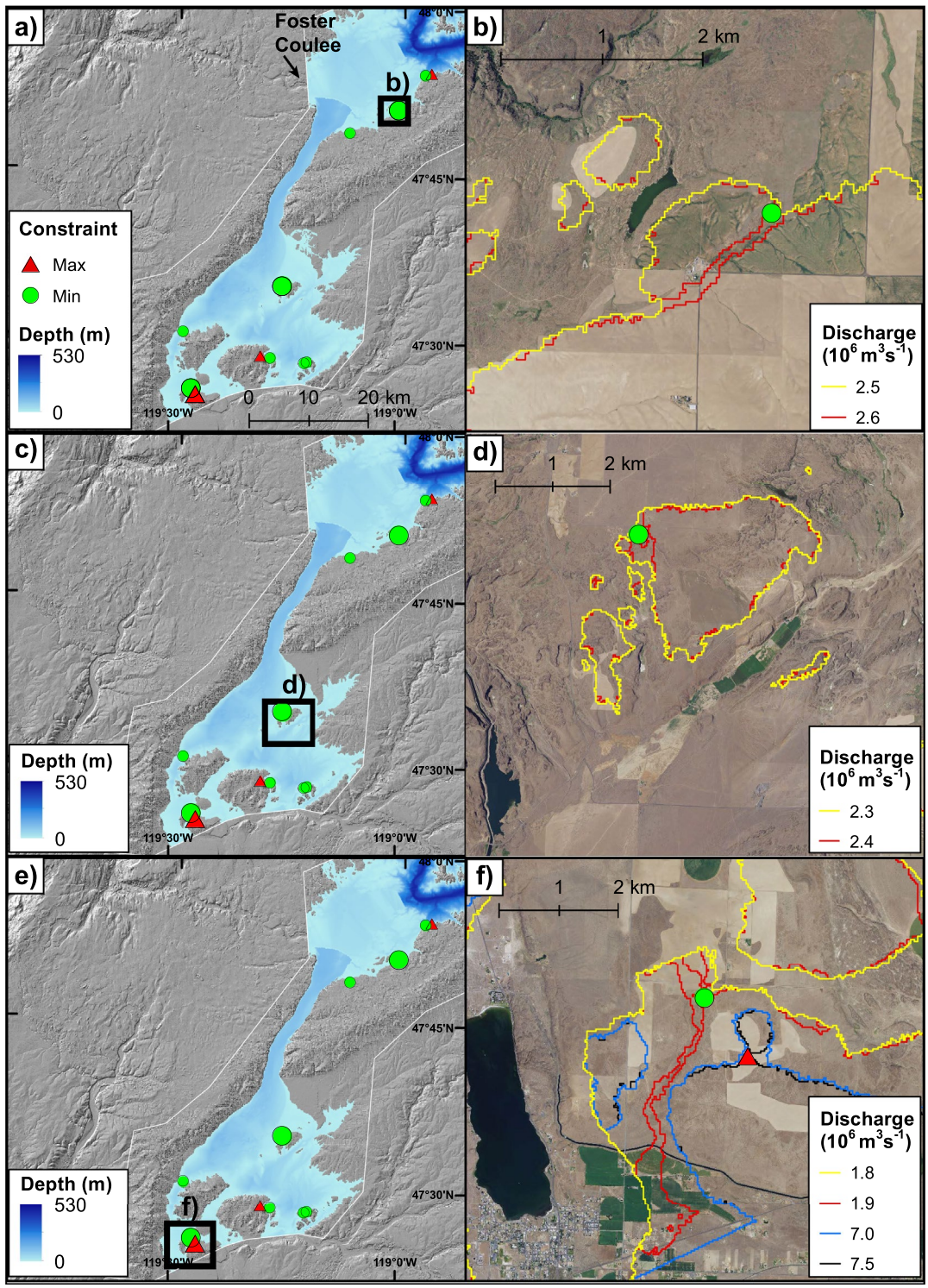

Figure 3. The high-water-inundating discharge for the cataract retreat scenario when water is permitted to exit the domain (white polygon) via Foster Coulee. (a) Depth of the 2.6×10^6 m^3 s^{-1} discharge, which is the minimum flow required to inundate the east rim high-water mark. (b) The drainage divide on the east rim (green circle) is crossed at a discharge of 2.6×10^6 m^3 s^{-1}. (c) Depth of the 2.4×10^6 m^3 s^{-1} discharge, which is the minimum flow required to inundate the high-water mark in Hartline basin. (d) The drainage divide on the Hartline bar (green circle) is crossed at a discharge of 2.4×10^6 m^3 s^{-1}. (e) Depth of the 1.9×10^6 m^3 s^{-1} discharge, which is the minimum flow required to inundate the divide that was crossed near the mouth of Lenore Canyon. (f) The drainage divide that constrains the minimum flood stage near the mouth of Lenore Canyon (green circle) is crossed at a discharge of 1.9×10^6 m^3 s^{-1}, while the maximum-constraint (drainage divide that was not flooded) is crossed at a discharge of 7.5×10^6 m^3 s^{-1}. The results are similar when flow is not permitted to exit via Foster Coulee, with somewhat smaller discharges inundating high-water marks in Hartline basin and at the mouth of Lenore Canyon (Figure S3 in Supporting Information S1).

3.3. Paleo-Discharge Inferred From the Present-Day Topography

The present-day topography scenario represents the post-incision state of the entire Grand Coulee canyon complex (Figure 2c). The high-water mark on the eastern rim is inundated at a discharge of 17×10^6 m^3 s^{-1} when Foster Coulee is open to flow (Figure 4), and at a discharge of 14×10^6 m^3 s^{-1} when flow is not permitted to exit the domain via Foster Coulee (Figure S12 in Supporting Information S1). The drainage divide at Hartline basin is crossed at a discharge of 6.5×10^6 m^3 s^{-1} with Foster Coulee open (Figure 4) and by the same value when it is closed to flow (Table 1). Simulations using a Manning's roughness coefficient of 0.04 rather than 0.065 predict inundation of the high-water mark on the eastern rim at a minimum discharge of 19×10^6 m^3 s^{-1}, and inundation of the Hartline Basin high-water mark at a minimum discharge of 7.5×10^6 m^3 s^{-1} when flow is allowed to exit through Foster Coulee (Figure S13 in Supporting Information S1).

3.4. Paleo-Discharge When Upper Grand Coulee Was Blocked by the Okanogan Lobe

When the Okanogan Lobe was at its maximum or near-maximum extent, the Withrow Moraine defined the southern limit of the ice margin, glacial features on Steamboat Rock defined the minimum eastward extent of the Okanogan Lobe (Bretz, 1932; Crosby & Carson, 1999), and deposition in glacial Lake Columbia indicates the inlet to upper Grand Coulee from the Columbia valley was blocked by ice (Atwater, 1986, 1987; Waitt & Thorson, 1983). The exact location of the ice margin in upper Grand Coulee is uncertain. There are erratics on the east rim, but they are presumed to be iceberg-rafted; till and striae, which are found on Steamboat Rock, have not been found on the east rim (Bretz, 1932). However, it has been proposed that floods were diverted into Northrup Canyon when upper Grand Coulee was blocked by ice (Balbas et al., 2017; Waitt, 2021). We therefore conservatively delineated the ice margin along the edge of upper Grand Coulee's eastern rim, leaving Northrup Canyon ice-free (Figure 2d). The modeled discharges that inundate the high scabland landscape on the east rim to the high-water marks are thus maximum values, as it is possible that the ice extended further east. These boundary conditions assume there was a static wall of ice that was not modified by floods.

High-water marks along the northeastern rim of upper Grand Coulee are inundated at a discharge of 0.45×10^6 m^3 s^{-1} when upper Grand Coulee is filled by ice (Figure 5). High-water marks further downstream are not inundated at this discharge, and most of the flow in lower Grand Coulee is routed through Lenore Canyon. Hence, any Missoula floods that may have occurred when upper Grand Coulee was occupied by the Okanogan Lobe would primarily have been routed through the Telford-Crab Creek and Cheney-Palouse tracts.

3.5. Paleo-Discharge Due to Drainage of Glacial Lake Columbia

We simulated two floods from glacial Lake Columbia draining into Grand Coulee (Figure 2e). The simulations are of an unsteady dam release flood due to instantaneous removal of the dam. Hence, the simulations represent the release of water from glacial Lake Columbia due to the erosion of the drainage divide at the Columbia valley by cataract retreat or collapse of an ice dam blocking the entrance of an already-incised upper coulee. The 750 m flood-swollen glacial Lake Columbia drainage model simulates a scenario where glacial Lake Columbia was swollen with an influx of floodwater from glacial Lake Missoula, as proposed by Atwater (1986) and is the maximum stage of glacial Lake Columbia. The 730 m-stage glacial Lake Columbia drainage scenario simulates the release of water from a longer-lived high-stand of glacial Lake Columbia (Atwater, 1986; Waitt & Thorson, 1983). We note that the stage of glacial Lake Columbia at the time of drainage through Grand Coulee is unknown, but drainage of both the 750 and 730 m-stage lake is geologically plausible. The lake extent was defined using the elevation associated with each stage (Atwater, 1986), with boundaries along the northern extent of the lake corresponding to mapped ice margins (Ehlers et al., 2011).

Inundating the Columbia valley upstream from Grand Coulee to 750 m elevation produced a lake 6,560 km^2 in area and 630 km^3 in volume, about 500 km^2 and 40 km^3 larger than values estimated by O'Connor et al. (2020). The peak discharge through the model domain with the present-day topography varied from 12.8×10^6 m^3 s^{-1} at the inlet of upper Grand Coulee to a total of 6.8×10^6 m^3 s^{-1} for the combined flow through all the outlets from

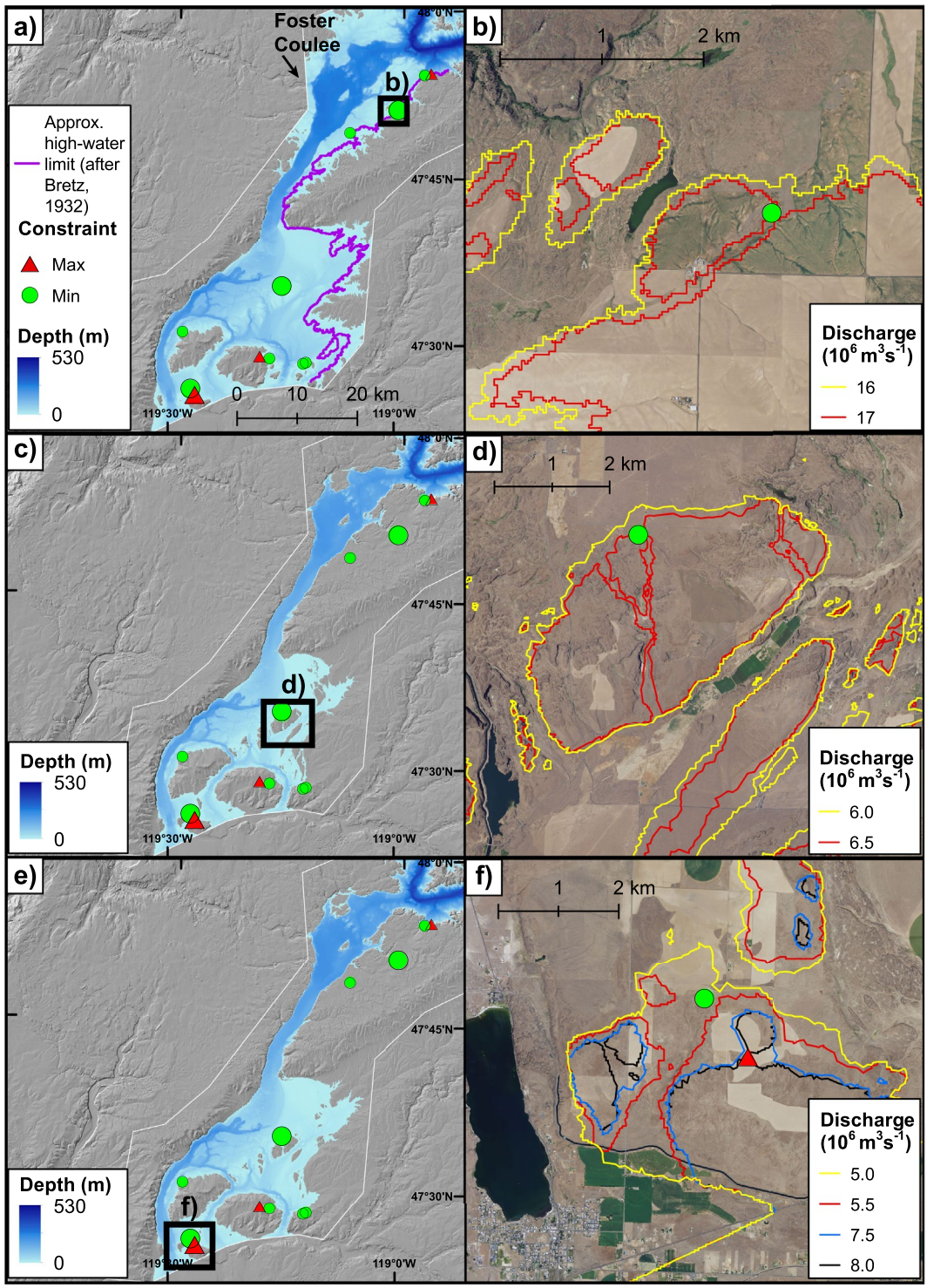

Figure 4. The high-water-inundating discharge for the present-day Grand Coulee scenario with Foster Coulee open to flow. (a) Depth of the 17×10^6 m^3 s^{-1} discharge, which is the minimum flow required to inundate the east rim high-water mark. (b) The drainage divide on the east rim (green circle) is crossed at a discharge of 17×10^6 m^3 s^{-1}. (c) Depth of the 6.5×10^6 m^3 s^{-1} discharge, which is the minimum flow required to inundate the high-water mark in Hartline basin. (d) The drainage divide on the Hartline bar (green circle) is crossed at a discharge of 6.5×10^6 m^3 s^{-1}. (e) Depth of the 5.5×10^6 m^3 s^{-1} discharge, which is the minimum flow required to inundate the divide that was crossed near the mouth of Lenore Canyon. (f) The drainage divide that constrains the minimum stage near the mouth of Lenore Canyon (green circle) is crossed at a discharge of 5.5×10^6 m^3 s^{-1}, while the maximum-constraint (drainage divide that was not flooded) is crossed at a discharge of 8.0×10^6 m^3 s^{-1}. Results when Foster Coulee is closed to flow are comparable, except the east rim high-water mark is crossed at a discharge of 14×10^6 m^3 s^{-1} (Figure S12 in Supporting Information S1).

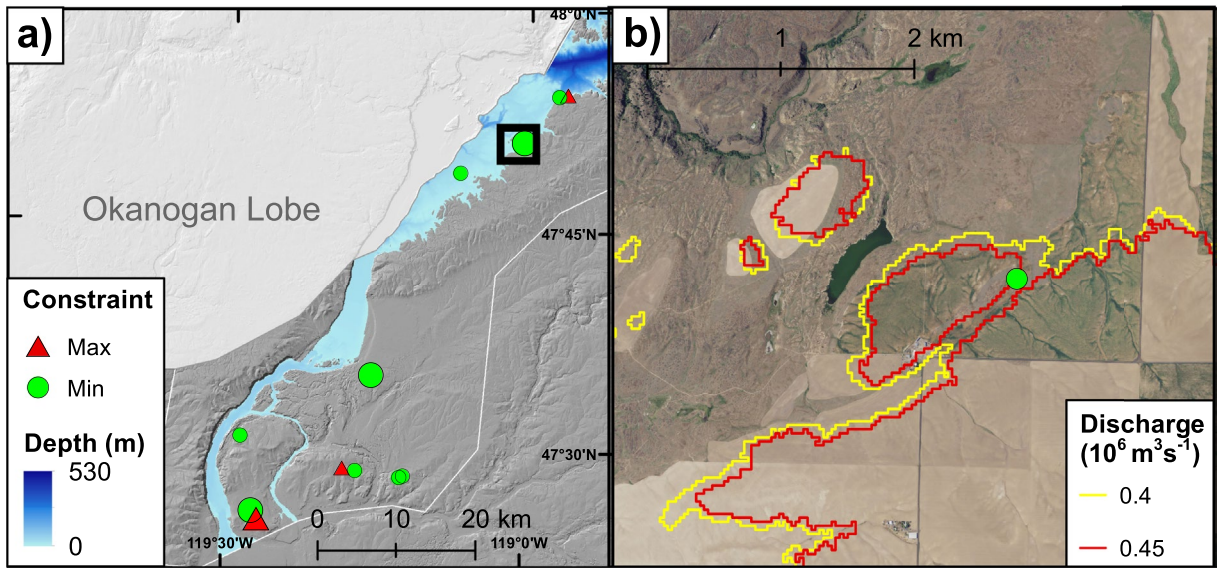

Figure 5. The high-water-inundating discharge for the model where upper Grand Coulee was blocked by ice from the Okanogan Lobe. (a) Depth of the 0.45 × 10^6 m^3 s^{-1} discharge, which is the minimum flow required to inundate the east rim high-water mark. (b) The drainage divide on the east rim (green circle) is crossed at a discharge of 0.45 × 10^6 m^3 s^{-1}.

lower Grand Coulee when Foster Coulee is closed. The discharge at the outlet is <1% lower when flow is allowed to exit the model domain via Foster Coulee (Figure 6, Figure S14 in Supporting Information S1). To average over instantaneous discharge fluctuations caused by unsteady flow conditions, we calculated peak discharge through 10 cross-sections near the high-water mark on the east rim where we evaluated steady-state discharge and found that the mean peak discharge is 7.6 × 10^6 m^3 s^{-1}, both when Foster Coulee is open and closed to flow (Figure 6, Figure S14 in Supporting Information S1). Results for the 730 m-stage lake draining flood are similar to those from the 750 m-stage simulation, with a mean peak discharge of 6.0 × 10^6 m^3 s^{-1} both when Foster Coulee is open (Figure S15 in Supporting Information S1) and closed to flow (Figure S16 in Supporting Information S1). Because the initial lake stage is higher than the eastern rim, the 750 m lake drainage inundates the northeastern rim upstream of Northrup Canyon, but the water drains through Northrup Canyon and does not inundate the rim further downstream. Hence, the discharge from draining the 750 m-stage glacial Lake Columbia does not inundate the high-water mark on the east rim, but the high-water mark in Hartline basin is inundated by the dam-release flood (Figure 6).

The flood draining from glacial Lake Columbia exhibits stage-discharge hysteresis (Figure 6b), consistent with unsteady, non-uniform floods caused by precipitation and dam failures (Altinakar et al., 2009; Graf & Qu, 2004). Hence, there are two possible discharges associated with a given flood stage, and at cross-sections proximal to the inlet from glacial Lake Columbia the peak discharge occurs at a stage that is tens of meters lower than the peak stage (Figures S17 and S18 in Supporting Information S1). For the same stage, discharge can vary by more than a factor of two (Figure 6b). The hysteresis results imply that even if paleo-flood stage is well-constrained, depending on the shape of the stage-discharge relation, there may still be uncertainties in the peak discharge reconstructed from high-water marks. The uncertainty would be greatest in cases where the peak stage and peak discharge are not simultaneous, and peak stage occurs at lower discharge than the peak value (Figure S19 in Supporting Information S1). Downstream from Grand Coulee, prior work has shown that flood stages in the hydraulically ponded Pasco, Yakima, and Umatilla basins were controlled by the discharge through the Columbia Gorge, such that higher discharge through the gorge leads to lower stages in the upstream basins (Denlinger et al., 2021). Hence, there can be complex relationships between stage and discharge that only emerge in dynamic models. Selecting reaches where critical or near-critical flow can be assumed (e.g., Baker, 1973; O'Connor & Baker, 1992) to reconstruct discharge from stage data reduces the likelihood that such complications influence paleo-discharge estimates. However, there may be cases, particularly if the flow was unsteady, where it may be challenging to estimate the Froude number of paleo-floods.

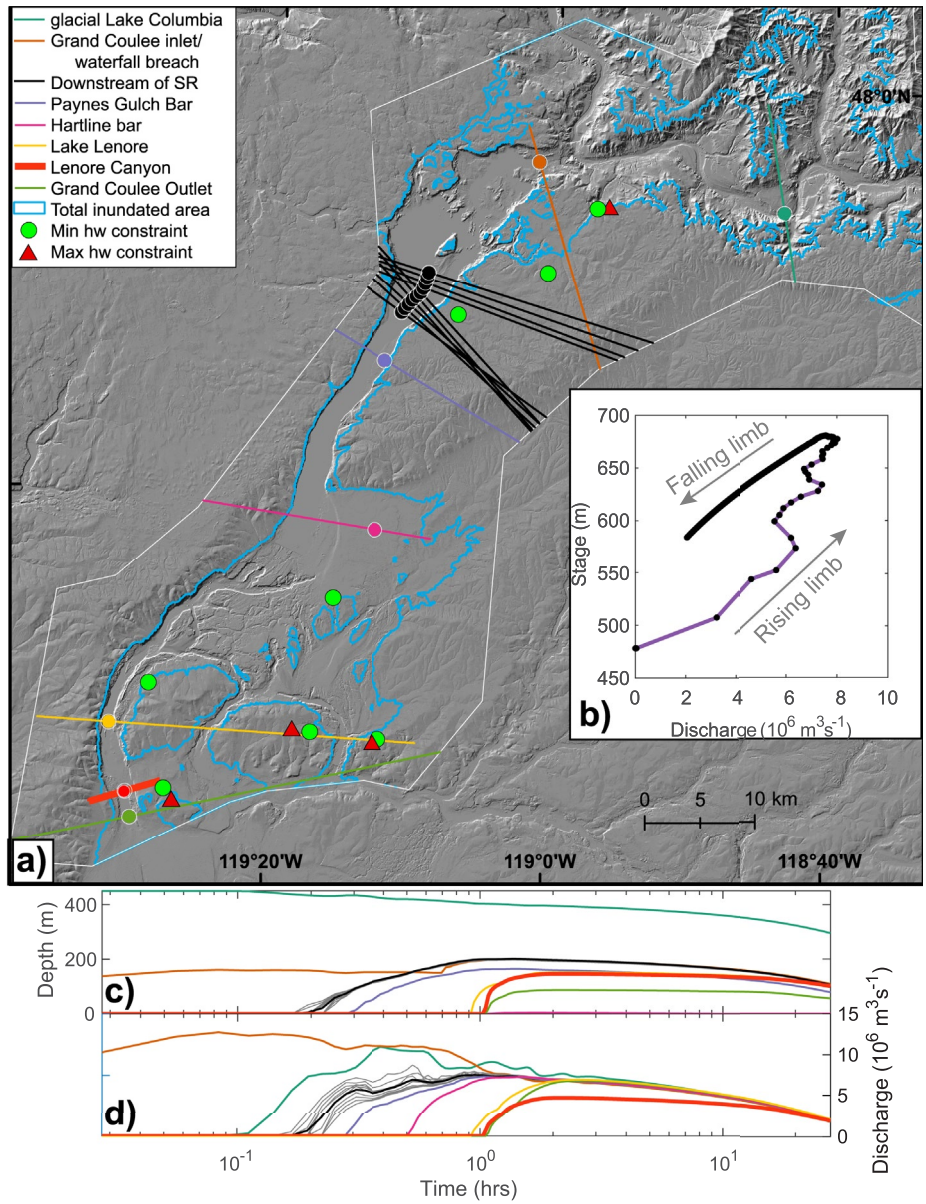

Figure 6. Flow depth, discharge, and flood inundation for drainage of a 750 m-stage glacial Lake Columbia (gLC) following instantaneous dam removal where flow can exit the domain (white polygon) via Foster Coulee. (a) The total extent of flood inundation. (b) Stage-discharge relationship for the 750 m flood-swollen gLC drainage at the middle of the 10 cross-sections downstream of Steamboat Rock (black lines). (c) Flow depth as a function of time for points on the cross-sections shown in panel (a). (d) Discharge as a function of time for cross-sections shown in panel (a). The results when Foster Coulee is closed to flow are similar (Figure S14 in Supporting Information S1), as are results when the initial lake stage is 730 m (Figures S15 and S16 in Supporting Information S1).

4. Thresholds for Cataract Retreat

Bretz (1923, 1924, 1932, 1969) recognized that erosion in the Channeled Scabland was dominated by plucking of the jointed and fractured Columbia River basalt, and that fluvial abrasion played a minor role. Field studies in other canyons confirm the dominance of plucking as the primary driver for erosion of fractured bedrock during floods (Anton et al., 2015; Baynes, Attal, Dugmore, et al., 2015; Baynes, Attal, Niedermann, et al., 2015; Beer et al., 2017; Lamb & Fonstad, 2010; Lamb et al., 2008, 2014; Malde, 1968). Many aspects of the mechanistic basis for plucking erosion have been investigated (Hurst et al., 2021; Lamb & Dietrich, 2009; Lamb et al., 2015; Lapotre et al., 2016), though other aspects, such as the role of interlocked joints, require further study (Lamb &

Dietrich, 2009). It has been suggested that the waterfalls in fractured basalt maintain vertical faces due to toppling of rock columns made of multiple blocks, which occurs due to the combined influence of shear stress generated by the overflowing water, buoyancy imparted by water in the plunge pool at the base of the waterfall, and gravity (Lamb & Dietrich, 2009). At Steamboat Rock, Bretz (1932, p. 48) inferred that "A receding waterfall mechanism would operate readily in the horizontal sheets of the Columbia basalt." Although we do not know the details of how cataract retreat progressed, given that the sides of Steamboat Rock are vertical or near-vertical escarpments of flood basalt, it is plausible that a column toppling mechanism drove retreat of the cataract through upper Grand Coulee. Hence, we assessed whether the shear stresses that were generated on the cataract brink by the high-water-inundating discharge would have been great enough to topple rock columns, using the torque balance model of Lamb and Dietrich (2009) modified to include wall cohesion between adjacent columns. We note that we do not use the toppling threshold to estimate paleo-discharge, as has been done in prior work (Larsen & Lamb, 2016), but rather assess whether the paleo-discharge constrained by field-based high-water evidence generated shear stresses that were great enough to topple columns and sustain headward cataract retreat.

The torques per unit width acting on a rectangular column of rock are due to gravity T_g, buoyancy T_b, fluid shear T_s, fluid drag T_d, and wall cohesion T_w:

$$T_g = \frac{1}{2} F_g L \cos\theta \left(1 - \frac{H}{L}\tan\theta\right) \tag{1}$$

$$T_b \approx \frac{1}{2} F_b L \tag{2}$$

$$T_s = F_s H \tag{3}$$

$$T_d = F_d H \tag{4}$$

$$T_w = \frac{1}{2} F_w H \tag{5}$$

where L is the horizontal column length (m), θ is the bed inclination (degrees), and H is the height of the toppling stack of columns (m), with respective forces F_g, F_b, F_s, F_d, and F_w calculated as:

$$F_g = \rho_r g L H \tag{6}$$

$$F_b \approx \rho g L H_p \tag{7}$$

$$F_s = \tau_o L \tag{8}$$

$$F_d = \frac{1}{2} \rho C_D U_\eta^2 \eta \tag{9}$$

$$F_w = \frac{2\tau_w H L w_{\text{frac}}}{W} \tag{10}$$

where ρ_r is the is the density of basalt (2,810 kg m^{-3}), g is gravitational acceleration (9.8 m s^{-2}), H_p is the plunge pool depth at the base of the waterfall (m), τ_o is the boundary shear stress over columns along the brink of the reconstructed waterfall (Pa), ρ is density of water (1,000 kg m^{-3}), C_D is a dimensionless local drag coefficient approximated as 1, a typical value for turbulent flows (Schlichting, 1979; Schmeeckle et al., 2007), U_η is the average flow velocity over the protruding column area (m s^{-1}), η is the block protrusion height (m), τ_w is the wall stress from the two laterally adjacent columns (Pa), w_{frac} is the fraction of the column surface that is interlocking with adjacent columns, and W is the horizontal column width (Lamb & Dietrich, 2009). A column of rock will topple when the driving torques exceed the resisting torques, resulting in a factor of safety FS less than 1, which we model with a modification of the Lamb and Dietrich (2009) approach to include a torque for wall cohesion:

$$\text{FS} = \frac{T_g - T_b + T_w}{T_s + T_d} \tag{11}$$

Substituting Equations 1–5 into Equation 11 and simplifying yields:

$$\mathrm{FS} = \frac{\cos\theta\left(1 - \frac{H}{L}\tan\theta\right) - \frac{\rho H_P}{\rho_r H} + \frac{2\tau_w w_{\mathrm{frac}}}{\rho_r g L}\frac{H}{W}}{\frac{\tau_o}{\rho g L}\left(2 + \frac{\rho C_D U_\eta^2}{\tau_o}\frac{\eta}{L}\right)} \tag{12}$$

and substituting $\tau_o = \rho u_*^2$ where u_* is the shear velocity, assuming $\tau_o = \tau_b$ allows us to rearrange and solve for τ_b as:

$$\frac{\tau_b}{\rho_r g L} = \frac{\frac{1}{2}\cos\theta\left(1 - \frac{H}{L}\tan\theta\right) - \frac{1}{2}\frac{\rho H_P}{\rho_r H} + \frac{\tau_w w_{\mathrm{frac}}}{\rho_r g L}\frac{H}{W}}{1 + \left(\frac{1}{2}C_D\left(\frac{U_\eta}{u_*}\right)^2\frac{\eta}{L}\right)} \tag{13}$$

where $(U_\eta/u_*)^2$ is 8.3, which is appropriate for hydraulically rough, turbulent flow (Lamb et al., 2015).

To estimate L, we measured the dimensions of basalt columns on Steamboat Rock. We measured 50 columns from a basalt flow with large columns near the base of Steamboat Rock along the southeast face and 153 columns across two locations on the summit. We used the median measured values to generate two estimates of L, one for each location, and assumed the columns were equant in plan view, such that W is equal to L. We calculated the height of the rock column H as the difference in the average elevation of the reconstructed cataract brink and the channel floor downstream from the brink. The plunge pool depth was calculated as the average water depth for the 2.6×10^6 m^3 s^{-1} discharge flood at distances between 10 and 150 m downstream from the brink. The median width (L) of 50 columns measured along the base of Steamboat Rock was 0.91 m, and the median column width of 153 columns measured at the top of Steamboat Rock was 0.68 m. The waterfall height was 192 m and the pool depth was 25.3 m (29.7 m for the 2.6×10^6 m^3 s^{-1} discharge with Foster Coulee closed to flow). θ was assumed to be equal to the gradient of the paleo-channel bed, which was estimated from the 10 m DEM to be 0.23° along the eastern bank of upper Grand Coulee, and η was estimated from field observations to be 0.1 m. Cohesion is expected to be greatest in the entablature portions of basalt flows (Baker, 2009). Field observations roughly constrain the entablature thickness to be 20% of the total thickness of basalt stratigraphy at Steamboat Rock, hence we assume a w_{frac} value of 0.2. A higher w_{frac} would result in a lower wall stress but require a higher fluid shear stress to topple the columns.

To estimate the wall stress τ_w from cohesive forces between adjacent columns, we first use the field measurements of column length and the height of the reconstructed cataract to identify geometrically unstable column stacks. A column of rock is geometrically unstable if the center of gravity lies outside the base (Hoek & Bray, 1981; Wyllie & Mah, 2004), as given by:

$$\frac{L}{H} < \tan\theta \tag{14}$$

A geometrically unstable column will not topple if the torque due to cohesion, T_w, is equal to or greater than the torque due to the weight of the column, such that $T_g \leq -T_w$, or written in terms of forces, $T_g \leq F_w r_w$, where T_g is the weight torque (N m), F_w is the cohesion force between columns (N), and r_w is the cohesion torque arm (m), assumed to be halfway up the column. We then perform a second torque balance on the geometrically unstable columns, assuming no flood-generated torques are present ($T_b = T_s = T_d = 0$); although cohesion may be similar among all columns in a given unit, only geometrically unstable columns require cohesion to exceed the gravitational torque to keep from toppling. Substituting Equations 1 and 6 for T_g and F_g yields the minimum cohesion force to hold a geometrically unstable column in place:

$$F_w = -\frac{\frac{1}{2}\rho_r g L^2 H\cos\theta\left(1 - \frac{H}{L}\tan\theta\right)}{r_w} \tag{15}$$

and the wall stress due to cohesion τ_w is calculated as the quotient of the cohesion force and the surface area of the column over which it acts, A_w, or:

$$\tau_w = \frac{F_w}{A_w} = \frac{F_w}{2 w_{\mathrm{frac}} \mathrm{HL}} \tag{16}$$

Equation 13 can then be solved for any length column, using the τ_w estimated from geometrically unstable columns.

Based on the assumptions described above, evaluating Equation 16 yields a median wall stress of 68 and 77 Pa for unstable columns measured at the base and top of Steamboat Rock, with median lengths of 0.58 and 0.55 m, respectively. The maximum wall stress values we infer from the measured lengths of unstable columns are 154 and 197 Pa, for columns at the base and top of Steamboat Rock, respectively. These are lower-bound estimates, since they are all based on intact rather than failed columns; the intact columns could be supported by greater cohesive stresses than the minimum required to balance gravitational torque. We note here that a column is not necessarily a vertical stack of basalt blocks bounded by cooling joints, which is what we measured in the field. Connectivity of larger-scale vertical joint sets that bound multiple inter-locked basalt blocks and extend through the entablature and between lava flows may define columns (e.g., Lamb & Dietrich, 2009). Columns with greater horizontal length (greater L) would require higher flood-generated shear stresses to topple, but are more likely to be geometrically stable.

Conceptually, the torque arm r_w may be set by the height of an interlocking section of adjacent columns, which could occur within a basalt flow entablature. Steamboat Rock is made up of multiple basalt flows, and since the position of the torque arm r_w is unknown, and likely complex, we simply assume an average position halfway up the column. If the position of the torque arm were higher or lower, a greater or lesser cohesive force, respectively, would be required to prevent the column from toppling.

We used Equation 13 to calculate a toppling threshold for the median, 25th percentile, 75th percentile, and 95th percentile column lengths measured at the base and top of Steamboat Rock, using both the median and the maximum wall stress. Using the median wall stress value of 68 Pa, the shear stress threshold required to topple the median length column at the base of Steamboat Rock was 867 Pa and thresholds for the 25th, 75th, and 95th percentile length columns were 325, 1,893, and 6,558 Pa respectively (using the maximum wall stress value of 154 Pa, toppling thresholds are 1,627 Pa for the median length column and 1,130, 2,604, and 7,160 Pa for the 25th, 75th, and 95th percentile length columns). For columns with lengths of those at the top of Steamboat Rock using the median wall stress value of 77 Pa, we calculated a threshold shear stress of 440 Pa required to topple the median length column and shear stresses of 266, 805, and 1,718 Pa required to topple the 25th, 75th, and 95th percentile length columns, respectively (using the maximum wall stress value of 197 Pa, toppling thresholds are 1,559 Pa for the median length column and 1,429, 1,878, and 2,725 Pa for the 25th, 75th, and 95th percentile length columns). The above values are for a pool depth of 25.3 m that forms for the 2.6×10^6 m^3 s^{-1} discharge that inundates the east rim high-water mark when Foster Coulee is open to flow. When Foster Coulee is closed to flow, the pool depth is 29.7 m and the threshold shear stresses for toppling are similar (Figure S20 in Supporting Information S1). Fluid pressure differences acting on the upstream and downstream sides of columns, as well as undercutting at the column base (which changes the location of the point where toppling columns pivot) or at larger scales (e.g., Baker & Nummedal, 1978)—neither of which we account for—would result in lower toppling thresholds (Hurst et al., 2021).

We calculate the shear stress along the cataract brink that was generated by the 2.6×10^6 m^3 s^{-1} discharge as (Lapotre & Lamb, 2015):

$$\tau = \rho C_f U^2 \tag{17}$$

where U is the modeled streamwise flow velocity (m s^{-1}) calculated from the vector sum of the x and y velocity components predicted by ANUGA, and $C_f = \frac{n^2 g}{h^{1/3}}$ is the friction coefficient (e.g., Stein & Julien, 1993), with Manning roughness coefficient n (0.065) and flow depth h (m). Although the distribution of shear stresses in bedrock canyons exhibits three-dimensional complexity (Venditti et al., 2014), the depth-averaged approach we use is commonly employed to quantify shear stresses generated at waterfalls (e.g., Lapotre & Lamb, 2015; Lapotre et al., 2016).

The median modeled shear stress for the high-water-inundating discharge of 2.6×10^6 m^3 s^{-1} is 876 Pa with 25th percentile 565 Pa, 75th percentile 1,329 Pa, and 95th percentile 2,345 Pa with Foster Coulee open (median of 839 Pa with 25th percentile 442 Pa, 75th percentile 1,400 Pa, and 95th percentile 2,481 Pa with Foster Coulee closed; Figure S20 in Supporting Information S1). The modeled shear stresses are of similar order to the thresholds for column toppling we predict from theory (Figure 7). The toppling theory is based on idealized columns and there is considerable uncertainty in the parameter values, especially cohesion. Additionally, turbulent fluctuations likely cause shear stresses to deviate several-fold from the mean value we model (Schmeeckle et al., 2007).

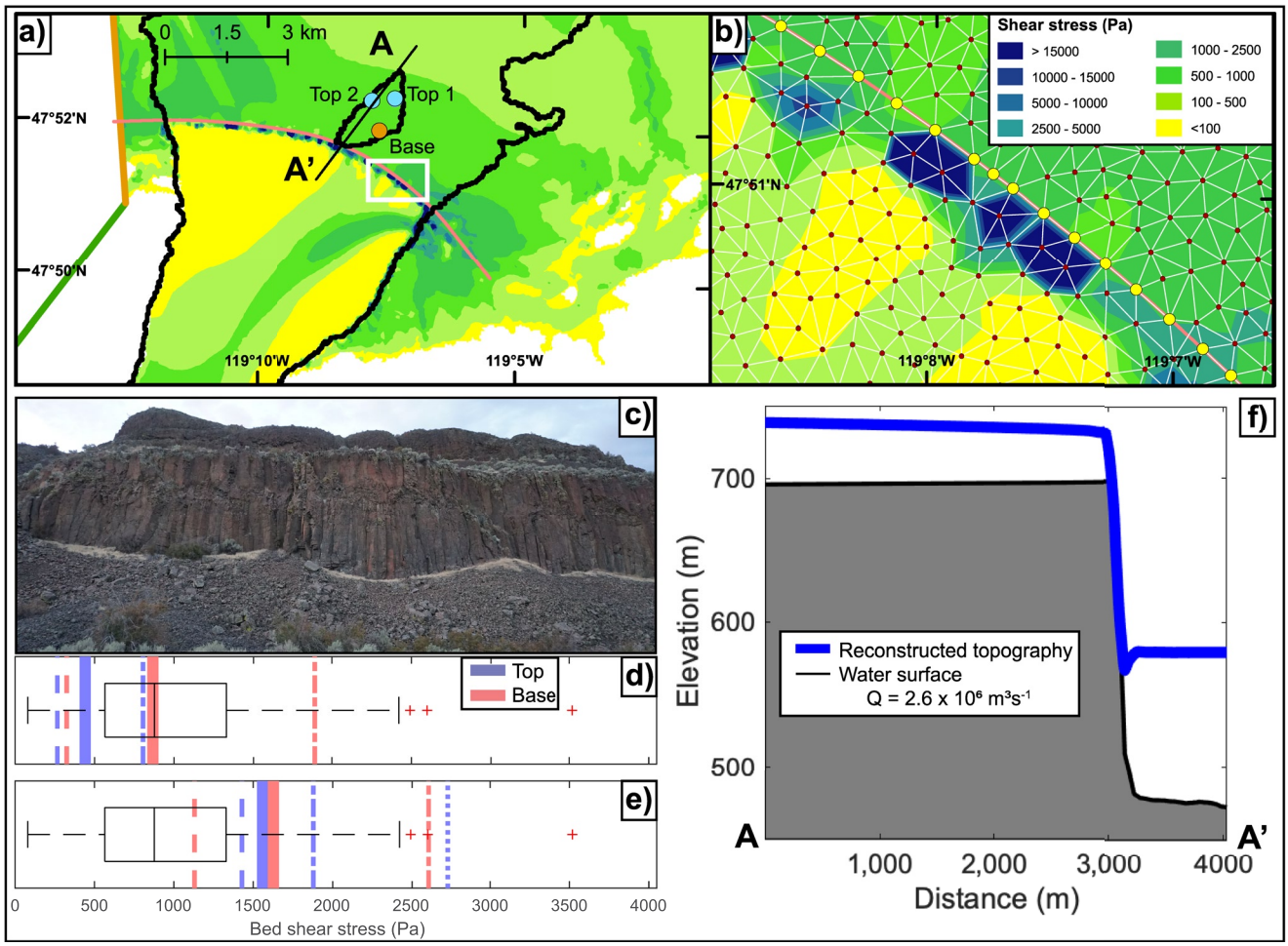

Figure 7. Plucking thresholds for the upper Grand Coulee cataract. (a) Map of shear stress for a discharge of 2.6×10^6 m^3 s^{-1} with Foster Coulee open to flow. The locations of column measurements are indicated by the orange and blue circles. (b) Close-up of the white box in panel (a) showing nodes (circles) and edges (white lines) of the computational mesh and the cataract brink (pink line). Modeled shear stresses at nodes along the brink of the reconstructed waterfall (large yellow circles) are used to generate the box plots in panels (d and e). (c) Photograph of the column measurement site near the base of Steamboat Rock. (d and e) Boxplots showing the distribution of shear stresses along the waterfall brink compared to the theory-based plucking thresholds using the median (d) and maximum (e) wall stress values with the median (solid lines), 25th (dashed lines), 75th (mixed dash-dot lines), and 95th (dotted lines) percentile horizontal lengths of unstable columns measured in the field. (f) Topographic and water surface profile from A to A′ which indicates there was free-falling water, rather than a submerged backward-facing step in upper Grand Coulee at the 2.6×10^6 m^3 s^{-1} discharge.

Despite these limitations, the agreement between the theory-based toppling shear stress thresholds and the hydraulic model-based shear stresses indicates that, to a first order, the smallest flood we predict that could have inundated the high-water mark on the eastern rim would have been sufficiently large to sustain cataract retreat by toppling columns.

5. Discussion

5.1. Paleo-Flood Magnitudes in Upper Grand Coulee

Our results indicate a discharge of 2.6×10^6 m^3 s^{-1} is most consistent with the high-water evidence in upper Grand Coulee prior to retreat of the cataract to the Columbia valley. The 2.6×10^6 m^3 s^{-1} discharge generates shear stresses on the cataract brink that exceed theory-based estimates of the threshold shear stress required to topple basalt columns, and hence is high enough to have plausibly sustained cataract retreat through upper Grand Coulee. These numerical findings are consistent with the accepted conceptual cataract retreat model of the formation of upper Grand Coulee (Bretz, 1932, 1969; O'Connor et al., 2020; Waitt et al., 2021) but further our

understanding by placing quantitative hydraulic constraints on the flood magnitude responsible for carving the largest canyon in the Channeled Scabland.

A discharge that caused canyon incision has been previously estimated for one other Channeled Scabland canyon: Moses Coulee, the second-largest canyon on the Columbia Plateau. Unlike the geologically constrained flow depth reconstructed for upper Grand Coulee, the flow depth in Moses Coulee was constrained using a mechanistic threshold shear stress model that assumed the canyon deepened when bed stresses exceeded the threshold for plucking (Larsen & Lamb, 2016). The discharge predicted for Moses Coulee ranged from 0.2–0.6 $\times$ 10^6 m^3 s^{-1}, with a value of 0.6 $\times$ 10^6 m^3 s^{-1} most consistent with depositional evidence (Larsen & Lamb, 2016). The canyon-carving discharge for Moses Coulee is 20% of the 3.0 $\times$ 10^6 m^3 s^{-1} discharge that fills the present-day topography to the high-water marks (Larsen & Lamb, 2016). Similarly, the 2.6 $\times$ 10^6 m^3 s^{-1} discharge responsible for the incision of upper Grand Coulee is approximately 15%–19% of the 14–17 $\times$ 10^6 m^3 s^{-1} discharge that fills the present-day topography of upper Grand Coulee to the high-water evidence. Though based on different discharge reconstruction methods, these findings indicate that modest-magnitude outburst flood discharges—with respect to those modeled using the present-day topography—were likely responsible for carving both canyons. In the case of Grand and Moses Coulees, the depth of the water spilling out of the Columbia valley and across the Waterville Plateau must have been relatively shallow, because the low-relief plateau surface lacks bedrock topography that could confine deep flows (Hanson, 1970; Waitt, 2021). Though it is possible loess could provide some degree of flow confinement, the relatively shallow flow depths (several tens of meters) of the canyon-carving discharges predicted for both Grand and Moses Coulees are consistent with the lack of substantial topographic confinement of flood flows. Collectively, these results indicate the two largest canyons in the Channeled Scabland were carved by floods with relatively modest discharges, which is consistent with other studies that have shown that relatively small-magnitude floods are capable of driving canyon incision via plucking of jointed bedrock (Anton et al., 2015; Baynes, Attal, Dugmore, et al., 2015; Lamb & Fonstad, 2010; van der Bilt et al., 2021). Hence, our findings are consistent with an inference first made by Bretz (1923, p. 644), who noted that higher flood deposits in the Channeled Scabland were abandoned when "deepening canyons drew the waters into more restricted routes."

5.2. Comparison Against Other Paleo-Discharge Estimates

The 14–17 $\times$ 10^6 m^3 s^{-1} steady-state discharge required to inundate the present-day topography to the high-water marks in upper Grand Coulee is slightly higher than, but of comparable magnitude to previous estimates that used high-water marks to estimate flow depth and discharge (Harpel, 1996; referenced in O'Connor et al., 2020; Harpel et al., 2000; Waitt et al., 2000, 2009, 2021). More recent work indicates floods produced by the failure of the ice dam impounding glacial Lake Missoula do not inundate the scabland on the east rim of upper Grand Coulee (Denlinger et al., 2021), indicating another scenario is required to explain the flood-scoured topography above the rim. We suggest the high-water marks were most likely emplaced when the cataract was retreating through the upper coulee (e.g., Waitt, 2021) or, alternatively, if the Okanogan Lobe forced flow out of glacial Lake Columbia onto the eastern rim when it blocked the coulee floor. It is also possible that the high-water marks were emplaced by a phase of flooding that pre-dates the blocking of the Columbia valley by the Okanogan Lobe, via overflow of hydraulically ponded floodwaters from the valley onto the Waterville Plateau. However, dynamic routing of Missoula floods suggest stages are not high enough to enter Grand Coulee without the Okanogan Lobe blocking the Columbia valley (O'Connor et al., 2020), hence this alternative is less likely. Future geochronology work may be able to distinguish among these multiple hypotheses.

The 14–17 $\times$ 10^6 m^3 s^{-1} steady discharges that inundate the east rim high-water mark on the present-day topography produce flood stages that exceed the high-water mark in Hartline basin mapped by Bretz (Bretz, 1932; Bretz et al., 1956). Given that the flood stages are incompatible with downstream geological evidence, this is further evidence that such high discharges likely did not occur. Our findings indicate the 2.6 $\times$ 10^6 m^3 s^{-1} discharge that eroded upper Grand Coulee by driving headward cataract retreat was <20% of that required to fill the canyon beyond the brim to the east rim high-water mark. The 7.6 $\times$ 10^6 m^3 s^{-1} outburst flood discharge from the drainage of glacial Lake Columbia measured near the east rim high-water mark is still only roughly half of the discharge that fills upper Grand Coulee to the high-water evidence. Hence, our results indicate flood magnitudes in upper Grand Coulee were considerably lower than those required to inundate the present-day canyon to the high-water marks. However, we acknowledge the possibility that the addition of discharge from a glacial Lake Missoula

flood, which we did not explicitly model, combined with a glacial Lake Columbia flood, could increase flood stages in Grand Coulee relative to our simulations that only drain a flood-swollen lake.

The maximum discharge for the model scenario with the floor of upper Grand Coulee blocked with ice was only 0.45×10^6 m^3 s^{-1}, indicating no large floods were traversing Grand Coulee when the Okanogan Lobe was at its maximum extent. The maximum 0.45×10^6 m^3 s^{-1} discharge we predict is greater than, but of similar magnitude to a 0.13×10^6 m^3 s^{-1} discharge estimate based on glacial Lake Columbia flood-bed sedimentology, although that value is inferred to be a minimum discharge estimate (Atwater, 1987). The flood-beds were deposited in upper Grand Coulee after the retreat of the cataract through the drainage divide, but when ice in the Columbia valley downstream from the inlet to Grand Coulee impounded a lower-stage glacial Lake Columbia (Atwater, 1987). The deposits are interpreted to represent later, low-magnitude Missoula floods (Atwater, 1987). Our results suggest low-magnitude floods could also have occurred slightly earlier, while the Okanogan lobe still blocked the coulee. However, whether the high-water marks on the eastern rim were emplaced by an earlier phase of flooding, during cataract retreat, or later when the Okanogan Lobe diverted flow out of glacial Lake Columbia is not resolvable by our methods. Geochronological constraints needed to make such a distinction are lacking; however, our result indicates that if floods were traversing upper Grand Coulee while the Okanogan Lobe blocked the coulee, they were likely relatively small.

Downstream at the transition between upper and lower Grand Coulee, Lapotre et al. (2016) inferred that discharge through the two main amphitheater heads of Dry Falls was $0.1–0.65 \times 10^6$ m^3 s^{-1}. Our simulations indicate modest discharges through upper Grand Coulee were large enough to inundate the falls; a discharge of 0.45×10^6 m^3 s^{-1} would have inundated not only the two main amphitheater heads, but nearly all of the ~6 km-wide falls (Figure 5a). Hence, it is possible that the morphology of Dry Falls is a geomorphic expression of later, smaller floods.

Although we focused our study on upper Grand Coulee and its mouth in Hartline basin, our results do provide some constraints on discharge in lower Grand Coulee, where a paleo-discharge of 4.5×10^6 m^3 s^{-1} was previously inferred near the mouth of Lenore Canyon (Baker, 1973). We compare our results against high-water evidence at two adjacent locations near the canyon mouth, one for a crossed divide and one for a divide that was not crossed by floodwaters (crossed divide, latitude: 47.42470, longitude: 119.45260, and elevation: 445 m; divide not crossed, latitude: 47.41620, longitude: 119.44260, and elevation: 463 m; Baker, 1973; O'Connor et al., 2020), that bracket the paleo-flood stage in Lenore Canyon. When the topography of Lenore Canyon is reconstructed to a pre-incision state, the lowest discharge that inundates the crossed divide is 1.9×10^6 m^3 s^{-1}, whereas a discharge of 5.5×10^6 m^3 s^{-1} exceeds the same high-water mark in the present-day topography (Table 1). The highest discharge that does not inundate the uncrossed divide when the lower Grand Coulee topography is reconstructed is 7.0×10^6 m^3 s^{-1}, whereas the highest discharge failing to cross the same divide on the present-day topography is 7.5×10^6 m^3 s^{-1}. The uncrossed divide requires much higher discharges to be inundated, but the values are not as well-constrained as for the crossed divide because we used larger discharge increments in the higher-discharge flood models. The peak discharge from the drainage of a 750 m-stage glacial Lake Columbia is 4.7×10^6 m^3 s^{-1} for a cross-section upstream from the high-water evidence in Lenore Canyon (Figure 6, thick red line). We note that the Quincy basin contained a hydraulically impounded backwater when floods were traversing Grand Coulee (Baker, 1973; Bretz, 1969), which is not incorporated in our simulations. Hence, it is possible that ponded water at the lower Grand Coulee mouth may have caused stage-discharge relationships to differ from those we predict. We also note that due to folding of the Coulee Monocline, the pre-incision topography of Lenore Canyon cannot be reconstructed by simply by interpolating between rims of canyons carved into flat-lying basalt, as is the case for reconstructing the cataract in upper Grand Coulee. Hence, our reconstructed topography and the discharge predicted for the pre-incision topography have a greater uncertainty in Lenore Canyon.

The 5.5×10^6 m^3 s^{-1} discharge we predict for the present-day topography that just exceeds the crossed divide near the mouth of Lenore Canyon is higher than, but of comparable magnitude to the prior 4.5×10^6 m^3 s^{-1} prediction from Baker (1973). The 4.7×10^6 m^3 s^{-1} peak discharge from the drainage of a 750 m-stage glacial Lake Columbia is very similar to the Baker (1973) estimate. However, there is substantial evidence of flood erosion in Lenore Canyon; Bretz (1932, p. 46) inferred Lenore Canyon was just a short gully prior to flooding and that it was cut entirely or greatly enlarged by flooding (Bretz, 1932, p. 68). Dry Falls and other topographic features such as the Great Blade, a long, thin butte that is >100 m taller than the surrounding landscape, provide evidence that retreating cataracts were responsible for incising Lenore Canyon. Baker (1978, p. 155) also inferred Lenore Canyon was carved by cataract recession. Without geochronologic control on the timing of the emplacement of the high-water

marks relative to individual floods, we cannot rule out that a large flood with a discharge of 4–5 × 10^6 m^3 s^{-1} emplaced the high-water evidence after Lenore Canyon had been incised. However, given Lenore Canyon formed by a similar cataract retreat mechanism as upper Grand Coulee, it is plausible and even likely the high-water evidence was emplaced prior to canyon incision and that our 1.9 × 10^6 m^3 s^{-1} estimate is representative of the flood magnitude that caused cataract retreat in Lenore Canyon. The 1.9 × 10^6 m^3 s^{-1} estimate is about 65% lower than the minimum discharge we infer would have inundated the crossed divide in the present-day topography and is about 58% lower than the prior estimate for Lenore Canyon (Baker, 1973). The lower and upper elevation constraints on flood stage near the mouth of Lenore Canyon differ in elevation by only 18 m, yet the difference in the discharge required to inundate them is several million m^3 s^{-1} (Figures 3 and 4, Figure S21 in Supporting Information S1) demonstrating that large increases in discharge can be required to achieve small increases in flood stage. Hence, stage-discharge relations (Figure S21 in Supporting Information S1) indicate even small amounts of erosion on the order of a few meters or tens of meters could cause discharge to be over-estimated if incision occurred after the high-water marks were emplaced and the post-flood topography was used to estimate flood stage.

5.3. Plucking Thresholds

Cohesion values for intact basalt estimated by the Hoek-Brown method are on the order of 66 MPa, with lower values of 0.6–6 MPa for columnar basalt rock masses (Schultz, 1995). Lower cohesion values ranging from 40 to 140 kPa have been reported for jointed and/or volcanic rock masses (Wyllie, 2017). These values are much higher than our estimates of minimum cohesion, which are on the order of tens to hundreds of Pa. Modeled shear stresses on the cataract brink are much lower than toppling thresholds predicted using cohesion values in the 10–100 kPa range. However, few studies have addressed the integrative influence of rock mass-scale strength (e.g., Schmidt & Montgomery, 1995) in columnar basalt. The presence of structural weaknesses in steep slopes can violate assumptions of the Hoek-Brown method, such that failure can occur under low stress conditions for short, steep slopes (Hoek & Brown, 1997). Column bases are not perfectly flat, nor are the edges of the columns perfectly angular, which also leads to ∼30% overestimates of cohesion (Alejano et al., 2015). Additionally, the lack of lateral confining stress along the downstream face of a retreating cataract would promote joint widening and reduce wall stresses (Lorig & Varona, 2001; Figure S22 in Supporting Information S1). If erosional unloading is required to generate joints that reduce basalt cohesion and hence permit cataract retreat, the joint development must occur rapidly. Observations of toppled columns in post-flood talus deposits (Figures S23 and S24 in Supporting Information S1), also indicate that failure can occur at stresses caused by near-surface weathering, without additional torque from flooding, which also suggests cohesive stresses are modest.

The failure stress of basalt columns has not been estimated in field experiments and as a result, there is still uncertainty regarding the incorporation of cohesive stresses into models of block toppling. However, even discharges that fill Channeled Scabland canyons to the brim with water fail to generate shear stresses that exceed 10 kPa (Larsen & Lamb, 2016), yet those canyons eroded by plucking (Bretz, 1923). Similarly, the Bonneville flood incised an entirely new course of the Snake River in an area where a basalt lava dam blocked the pre-flood river channel (O'Connor, 1993; Scott et al., 1982). The Bonneville flood had a peak discharge of 1 × 10^6 m^3 s^{-1} at Red Rock Pass, which attenuated downstream, and generated shear stresses of about 1–3 kPa in constricted reaches (O'Connor, 1993). The Bonneville flood also drove km-scale retreat of cataracts up to ∼100 m in height where floodwaters re-entered the Snake River canyon after over-topping the canyon brim and flowing on the adjacent uplands (Malde, 1968). The cataract retreat would have been driven by a small fraction of the total flood discharge. Abundant boulder deposits along the Snake River are attributed to the rounding of basalt columns that were plucked and transported by the Bonneville flood (Malde, 1968).

The findings from the Bonneville flood indicate extensive basalt plucking and cataract retreat can occur at discharges lower than we predict for upper Grand Coulee and at shear stresses of only a few kPa, which overlaps with the range of shear stresses we predict on the upper Grand Coulee cataract brink. Hence, although our estimates of basalt cohesion are lower than existing examples, they are consistent with geomorphic evidence of erosion via plucking and reconstructed flood hydraulics (Larsen & Lamb, 2016; O'Connor, 1993).

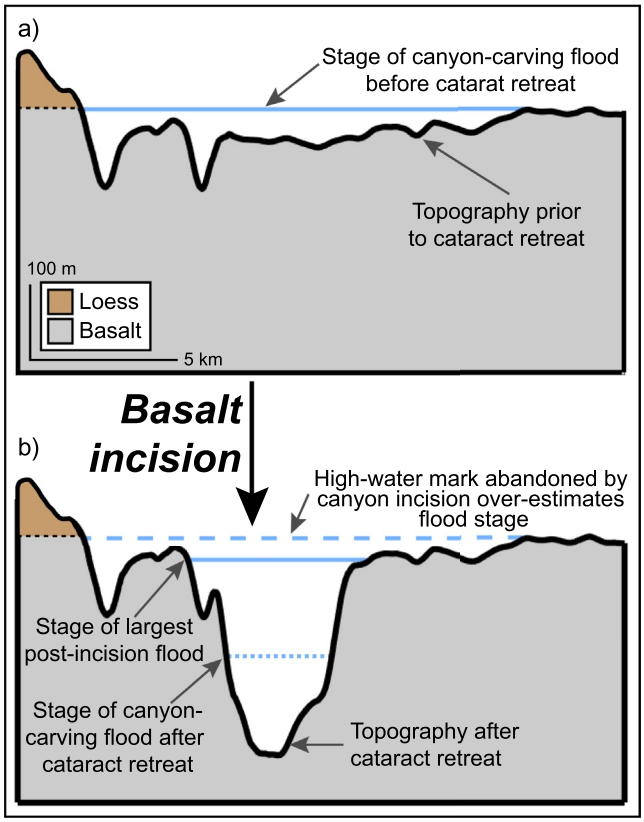

Figure 8. Conceptualization of the co-evolution of topography and flood stage in canyons eroded primarily by waterfall or cataract retreat. (a) Flow depths are low for the channel upstream from the cataract brink. (b) The water surface elevation decreases after the cataract retreats upstream. In the case of upper Grand Coulee, floods that occurred following cataract retreat produced higher stages, but did not reach the elevation of high-water marks formed by an earlier flood. The change in water surface elevation is conceptually similar for flood channels that did not erode by cataract retreat, though the magnitude of the change would be less. Cross section location is at the upstream-most extent of topographic reconstruction, and indicated as A–A′ in Figures S17e and S18e in Supporting Information S1.

5.4. Implications for Paleo-Discharge Reconstruction

Beyond Grand Coulee, there are prominent examples of incision by cataract retreat in the Channeled Scabland. Large-scale cataract retreat occurred at Moses Coulee, Drumheller Channels, Devil's Canyon, Palouse Falls, Potholes Coulee, and Frenchman Coulee, and paleo-water surface profiles and discharge have been predicted by different means in some of these areas (e.g., Baker, 1973; Hanson, 1970; Larsen & Lamb, 2016; Lapotre et al., 2016). Other channels where cataract retreat did not occur have also been targets for paleo-flood reconstruction because the magnitude of flood-induced erosion was lower, and is therefore less of a complicating factor (e.g., Baker, 1973; Benito & O'Connor, 2003; O'Connor & Baker, 1992). Prior studies that routed glacial Lake Missoula floodwaters across the entire Channeled Scabland have suggested that a flood with three times the water volume of glacial Lake Missoula is required to match high-water marks in the Channeled Scabland (Komatsu et al., 2000; Miyamoto et al., 2007). More recent 2D modeling has not reached a similar conclusion (Denlinger & O'Connell, 2010; Denlinger et al., 2021), though there are still discrepancies between modeled flood stage and field-based high-water evidence (Denlinger et al., 2021; O'Connor et al., 2020). Multiple factors may explain the mismatch between field evidence and modeled inundation extents, but one factor that could explain the mismatch in some areas is that erosion of channel floors or walls causes flood stages to lower relative to high-water marks (Figure 8). For example, our results from upper Grand Coulee indicate the water surface elevation dropped by ∼150 m following retreat of the cataract (Figure 7f). The drop of water surface elevation would have been less in those areas that did not undergo incision by cataract retreat, but incision still may have been great enough to generate elevation changes on the order of meters to tens of meters. The uncertainty and spatial variability of Manning's roughness may also contribute to the mismatch, with simulations using a smaller roughness coefficient of 0.04 yielding stages 0%–3% lower than those which use a roughness of 0.065, and requiring discharges about 10%–25% higher to inundate a given high-water mark (Figure S25 in Supporting Information S1). Areas where the Missoula floods were flowing over granite, such as in the Columbia valley downstream from the inlet to Grand Coulee (Waitt, 2016, 2021) may have experienced less erosion than areas where floods were flowing across jointed basalt; hence high-water marks there may provide more accurate constraints on peak discharge. However, detailed investigations of flood-induced erosion in such areas are lacking, and assessment of erosion is required because fractured granite can be plucked and rapidly eroded similarly to fractured and jointed basalt (e.g., Anton et al., 2015).

Attempts to reconstruct discharge for large channels on Mars have commonly estimated flow depth by assuming the channels were filled to their brims with water (e.g., Baker, 2001; Burr, 2003; Burr et al., 2002; Komatsu & Baker, 1997). Topographic evidence indicates large knickpoints retreated through major channels on Mars (Baker, 1982; Baker & Kochel, 1979; Duran & Coulthard, 2020; Duran et al., 2019; Warner et al., 2010, 2013). Our analysis of Grand Coulee indicates the discharge prior to knickpoint passage was approximately six times lower than the discharge required to fill the present-day canyon to the elevation of high-water marks, which are located near the elevation of the canyon brim. Given the evidence for large-scale cataract retreat, our results suggest assuming brimful flow could lead to over-estimation of paleo-discharge in channels on Mars (e.g., Larsen & Lamb, 2016). Such a mechanism should be investigated, as others have suggested flow rates through the aquifers thought to have sourced the floods on Mars are too low to produce discharges that fill channels brimful with water (e.g., Andrews-Hanna & Phillips, 2007; Manga, 2004) and that assuming brimful flow causes discharge to be over-estimated by up to a factor of 25 (Wilson et al., 2004).

6. Conclusions

We reconstructed paleo-flood discharge for upper Grand Coulee, eastern Washington, USA, which was carved by Pleistocene megafloods from the catastrophic drainage of glacial Lake Missoula. Grand Coulee is the largest canyon in the Channeled Scabland and has geomorphic characteristics comparable to larger and older channels on Mars. Geological high-water evidence and hydraulic modeling indicate the discharge upstream of a waterfall or cataract that retreated through upper Grand Coulee was 2.6×10^6 m^3 s^{-1}. The 2.6×10^6 m^3 s^{-1} discharge produces shear stresses on the waterfall brink that exceed theory-based plucking thresholds for toppling rock columns. Hence, the relatively modest discharge we predict was sufficient to sustain cataract retreat. The largest flood through upper Grand Coulee, which could have been triggered if the stage of glacial Lake Columbia was 750 m when the cataract retreated through the divide separating upper Grand Coulee and the Columbia valley or when an ice dam failed, has an estimated discharge of 7.6×10^6 m^3 s^{-1}. Later, when upper Grand Coulee was blocked by the Okanogan Lobe of the Cordilleran Ice Sheet, the maximum discharge would have been 0.45×10^6 m^3 s^{-1} if the ice sheet forced floods onto the eastern canyon rim, which is of comparable magnitude to prior estimates for late, waning-phase Missoula floods. The discharge that drove cataract retreat is 81%–86% lower than the $14–17 \times 10^6$ m^3 s^{-1} discharge that inundates the same high-water marks for floods routed across the present-day topography. The discharge that drove cataract retreat is also only one-third of the magnitude of the peak discharge predicted by a dam release flood from glacial Lake Columbia, which is an estimate of the highest discharge that could have been routed through upper Grand Coulee. Our findings highlight the need to account for erosion when reconstructing discharge in flood-eroded landscapes, as lowering of channel floors can cause flood stages to drop below the elevation of high-water marks, leading to overestimation of paleo-flow depth, which has implications for interpreting paleo-discharge and hydrology from bedrock channel morphology. We find that discharges substantially lower than those required to fill canyons with water were capable of incising deep bedrock canyons in the Channeled Scabland. Our findings are consistent with studies that indicate low-to moderate-magnitude floods are capable of eroding canyons in fractured bedrock. If channels on Mars incised via cataract retreat, assuming they were filled to the brim with water could lead to over-estimation of discharge.

Data Availability Statement

All code, input, and output files are archived at the University of Massachusetts Amherst Library data repository (https://doi.org/10.7275/j72g-rx55).

Acknowledgments
The authors would like to thank Evan Thaler, Scott David, and Michael Lamb for helpful conversations and Scott David, Madison Douglas, and Michael Lamb for assistance with fieldwork. The authors thank Michael Lamb for insight and advice on incorporating cohesion into the column toppling model. The authors thank Victor Baker, Tao Liu, Jeremy Venditti, and three anonymous reviewers for helpful reviews, Editor Amy East and Associate Editor Jon Pelletier for constructive comments, and Jim O'Connor for helpful feedback. The authors also thank the co-leaders and participants of the 2021 Geological Society of America field trip to upper Grand Coulee for stimulating conversations. The authors also acknowledge the historical and present significance of the Grand Coulee region to the Confederated Tribes of the Colville Reservation—composed of members of the Chelan, Nez Perce, Colville, Entiat, Lakes, Methow, Moses-Columbia, Nespelem, Okanogan, Palus, San Poil, and Wenatchi tribes. This work was supported by an NSF Graduate Research Fellowship to K. E. Lehnigk, and the NSF Grant 1529110 to I. J. Larsen.

References

Alejano, L. R., Carranza-Torres, C., Giani, G. P., & Arzúa, J. (2015). Study of the stability against toppling of rock blocks with rounded edges based on analytical and experimental approaches. *Engineering Geology*, *195*, 172–184. https://doi.org/10.1016/j.enggeo.2015.05.030

Altinakar, M. S., Matheu, E. E., & McGrath, M. Z. (2009). *New generation modeling and decision support tools for studying impacts of dam failures* (Technical Report). Association of State Dam Safety Officials (ASDSO).

Andrews-Hanna, J. C., & Phillips, R. J. (2007). Hydrological modeling of outflow channels and chaos regions on Mars. *Journal of Geophysical Research: Planets*, *112*(E8). https://doi.org/10.1029/2006JE002881

Anton, L., Mather, A. E., Stokes, M., Muñoz-Martin, A., & De Vicente, G. (2015). Exceptional river gorge formation from unexceptional floods. *Nature Communications*, *6*(1), 1–11. https://doi.org/10.1038/ncomms8963

Atwater, B. F. (1984). Periodic floods from glacial Lake Missoula into the Sanpoil arm of glacial Lake Columbia, northeastern Washington. *Geology*, *12*(8), 464–467. https://doi.org/10.1130/0091-7613(1984)12<464:pffglm>2.0.co;2

Atwater, B. F. (1986). Pleistocene glacial-lake deposits of the Sanpoil River valley, northeastern Washington. *U.S. Geological Survey Bulletin*, *1661*. https://doi.org/10.3133/b1661

Atwater, B. F. (1987). Status of glacial Lake Columbia during the last floods from glacial Lake Missoula. *Quaternary Research*, *27*(2), 182–201. https://doi.org/10.1016/0033-5894(87)90076-7

Baker, V. R. (1973). Paleohydrology and sedimentology of Lake Missoula flooding in Eastern Washington. *Geological Society of America Special Papers*, *144*(79), 1–73. https://doi.org/10.1130/SPE144-p1

Baker, V. R. (1978). Large-scale erosional and depositional features of the Channeled Scabland. In V. R. Baker & D. Nummedal (Eds.), *The Channeled Scabland* (pp. 81–115). NASA Office of Space Science, Planetary Geology Program.

Baker, V. R. (1979). Erosional processes in channelized water flows on Mars. *Journal of Geophysical Research*, *84*(B14), 7985–7993. https://doi.org/10.1029/JB084iB14p07985

Baker, V. R. (1982). *The channels of Mars* (p. 198). University of Texas Press.

Baker, V. R. (2001). Water and the Martian landscape. *Nature*, *412*(6843), 228–236. https://doi.org/10.1038/35084172

Baker, V. R. (2002). The study of superfloods. *Science*, *295*(5564), 2379–2380. https://doi.org/10.1126/science.1068448

Baker, V. R. (2008). Greatest floods and largest rivers. In A. Gupta (Ed.), *Large rivers: Geomorphology and management* (pp. 65–74). https://doi.org/10.1002/9780470723722.ch5

Baker, V. R. (2009). The Channeled Scabland: A retrospective. *Annual Review of Earth and Planetary Sciences*, *37*, 393–411. https://doi.org/10.1146/annurev.earth.061008.134726

Baker, V. R., & Kochel, R. C. (1979). Martian channel morphology: Maja and Kasei Valles. *Journal of Geophysical Research*, *84*(B14), 7961–7983. https://doi.org/10.1029/JB084iB14p07961

Baker, V. R., & Milton, D. J. (1974). Erosion by catastrophic floods on Mars and Earth. *Icarus*, *23*(1), 27–41. https://doi.org/10.1016/0019-1035(74)90101-8

Baker, V. R., & Nummedal, D. (1978). *The Channeled Scabland: A guide to the geomorphology of the Columbia Basin, Washington* (p. 186). NASA.

Baker, V. R., Strom, R. G., Gulick, V. C., Kargel, J. S., Komatsu, G., & Kale, V. S. (1991). Ancient oceans, ice sheets and the hydrological cycle on Mars. *Nature*, *352*(6336), 589–594. https://doi.org/10.1038/352589a0

Balbas, A. M., Barth, A. M., Clark, P. U., Clark, J., Caffee, M., O'Connor, J., et al. (2017). ^{10}Be dating of late Pleistocene megafloods and Cordilleran Ice Sheet retreat in the northwestern United States. *Geology*, *45*(7), 583–586. https://doi.org/10.1130/G38956.1

Barber, D. C., Dyke, A., Hillaire-Marcel, C., Jennings, A. E., Andrews, J. T., Kerwin, M. W., et al. (1999). Forcing of the cold event of 8,200 years ago by catastrophic drainage of Laurentide lakes. *Nature*, *400*(6742), 344–348. https://doi.org/10.1038/22504

Barry, T. L., Kelley, S. P., Reidel, S. P., Camp, V. E., Self, S., Jarobe, N. A., et al. (2013). Eruption chronology of the Columbia River Basalt Group. In S. P. Reidel, V. E. Camp, M. E. Ross, J. A. Wolff, B. S. Martin, T. L. Tolan, & R. E. Wells (Eds.), *The Columbia River flood basalt province: Geological Society of America Special Papers* (Vol. 497, pp. 45–66). https://doi.org/10.1130/2013.2497(02)

Baynes, E., Attal, M., Dugmore, A. J., Kirstein, L. A., & Whaler, K. A. (2015). Catastrophic impact of extreme flood events on the morphology and evolution of the lower Jökulsá á Fjöllum (northeast Iceland) during the Holocene. *Geomorphology*, *250*, 422–436. https://doi.org/10.1016/j.geomorph.2015.05.009

Baynes, E., Attal, M., Niedermann, S., Kirstein, L. A., Dugmore, A. J., & Naylor, M. (2015). Erosion during extreme flood events dominates Holocene canyon evolution in northeast Iceland. *Proceedings of the National Academy of Sciences*, *112*(8), 2355–2360. https://doi.org/10.1073/pnas.1415443112

Beer, A. R., Turowski, J. M., & Kirchner, J. W. (2017). Spatial patterns of erosion in a bedrock gorge. *Journal of Geophysical Research: Earth Surface*, *122*(1), 191–214. https://doi.org/10.1002/2016JF003850

Benito, G., & O'Connor, J. E. (2003). Number and size of last-glacial Missoula floods in the Columbia River valley between the Pasco Basin, Washington, and Portland, Oregon. *Geological Society of America Bulletin*, *115*(5), 624–638. https://doi.org/10.1130/0016-7606(2003)115<0624:nasolm>2.0.co;2

Benito, G., & Thorndycraft, V. R. (2020). Catastrophic glacial-lake outburst flooding of the Patagonian Ice Sheet. *Earth-Science Reviews*, *200*, 102996. https://doi.org/10.1016/j.earscirev.2019.102996

Bjornstad, B., & Kiver, E. (2012). *On the trail of the ice age floods the northern reaches: A geological field guide to northern Idaho and the Channeled Scabland* (p. 432). Keokee Books.

Bretz, J. H. (1923). The Channeled Scablands of the Columbia Plateau. *The Journal of Geology*, *31*(8), 617–649. https://doi.org/10.1086/623053

Bretz, J. H. (1924). The Dalles type of river channel. *The Journal of Geology*, *32*(2), 139–149. https://doi.org/10.1086/623074

Bretz, J. H. (1932). *The Grand Coulee* (Special Publication No. 15). American Geographical Society.

Bretz, J. H. (1969). The Lake Missoula floods and the Channeled Scabland. *The Journal of Geology*, *77*(5), 505–543. https://doi.org/10.1086/627452

Bretz, J. H., Smith, H. T. U., & Neff, G. E. (1956). Channeled Scabland of Washington: New data and interpretations. *Geological Society of America Bulletin*, *67*(8), 957–1049. https://doi.org/10.1130/0016-7606(1956)67[957:CSOWND]2.0.CO;2

Burr, D. M. (2003). Hydraulic modelling of Athabasca Vallis, Mars. *Hydrological Sciences Journal*, *48*(4), 655–664. https://doi.org/10.1623/hysj.48.4.655.51407

Burr, D. M., Grier, J. A., McEwen, A. S., & Keszthelyi, L. P. (2002). Repeated aqueous flooding from the Cerberus Fossae: Evidence for very recently extant, deep groundwater on Mars. *Icarus*, *159*(1), 53–73. https://doi.org/10.1006/icar.2002.6921

Carling, P. A. (1996). Morphology, sedimentology and paleohydraulic significance of large gravel dunes: Altai Mountains, Siberia. *Sedimentology*, *43*(4), 647–664. https://doi.org/10.1111/j.1365-3091.1996.tb02184.x

Carr, M. (1979). Formation of Martian flood features by release of water from confined aquifers. *Journal of Geophysical Research*, *84*(B6), 2995–3007. https://doi.org/10.1029/jb084ib06p02995

Clark, P. U., Marshall, S. J., Clarke, G. K. C., Hostetler, S. W., Licciardi, J. M., & Teller, J. T. (2001). Freshwater forcing of abrupt climate change during the last glaciation. *Science*, *293*(5528), 283–287. https://doi.org/10.1126/science.1062517

Clarke, G. K. C., Mathews, W. H., & Pack, R. T. (1984). Outburst floods from glacial Lake Missoula. *Quaternary Research*, *22*(3), 289–299. https://doi.org/10.1016/0033-5894(84)90023-1

Condron, A., Joyce, A. J., & Bradley, R. S. (2020). Arctic sea ice export as a driver of deglacial climate. *Geology*, *48*(4), 395–399. https://doi.org/10.1130/G47016.1

Cook, K. L., Andermann, C., Gimbert, F., Adhikari, B. R., & Hovius, N. (2018). Glacial lake outburst floods as drivers of fluvial erosion in the Himalaya. *Science*, *362*(6410), 53–57. https://doi.org/10.1126/science.aat4981

Crosby, C. J., & Carson, R. J. (1999). The geology of Steamboat Rock, Grand Coulee, Washington. *Washington Geology*, *27*(2/3/4), 3–8.

Denlinger, R. P., George, D. L., Cannon, C. M., O'Connor, J. E., & Waitt, R. B. (2021). Diverse cataclysmic floods from Pleistocene glacial Lake Missoula. In R. B. Waitt, G. D. Thackray, & A. R. Gillespie (Eds.), *Untangling the Quaternary period—A legacy of Stephen C. Porter: Geological Society of America Special Papers* (Vol. 548). https://doi.org/10.1130/2021.2548(17)

Denlinger, R. P., & O'Connell, D. R. H. (2010). Simulations of cataclysmic outburst floods from Pleistocene glacial Lake Missoula. *Geological Society of America Bulletin*, *122*(5), 678–689. https://doi.org/10.1130/B26454.1

Duran, S., & Coulthard, T. J. (2020). The Kasei Valles, Mars: A unified record of episodic channel flows and ancient ocean levels. *Scientific Reports*, *10*(1), 1–7. https://doi.org/10.1038/s41598-020-75080-y

Duran, S., Coulthard, T. J., & Baynes, E. R. C. (2019). Knickpoints in Martian channels indicate past ocean levels. *Scientific Reports*, *9*(1), 1–6. https://doi.org/10.1038/s41598-019-51574-2

Ehlers, J., Gibbard, P. L., & Hughes, P. D. (2011). *Quaternary glaciations—extent and chronology: A closer look* (Vol. 15). Elsevier.

Ferrari, R. L. (2012). *Franklin D. Roosevelt Lake—Grand Coulee Dam 2010-11 Survey*. (Technical Report No. SRH-2012-06). U.S. Bureau of Reclamation Technical Service Center.

Garcia-Castellanos, D., & O'Connor, J. E. (2018). Outburst floods provide erodability estimates consistent with long-term landscape evolution. *Scientific Reports*, *8*(1), 1–9. https://doi.org/10.1038/s41598-018-28981-y

Goudge, T. A., & Fassett, C. I. (2018). Incision of Licus Vallis, Mars, from multiple lake overflow floods. *Journal of Geophysical Research: Planets*, *123*(2), 405–420. https://doi.org/10.1002/2017JE005438

Graf, W. H., & Qu, Z. (2004). Flood hydrographs in open channels. *Proceedings of the Institution of Civil Engineers - Water Management*, *157*(WMI), 45–52. https://doi.org/10.1680/wama.2004.157.1.45

Gupta, S., Collier, J. S., Palmer-Felgate, A., & Potter, G. (2007). Catastrophic flooding origin of shelf valley systems in the English Channel. *Nature*, *448*(7151), 342–345. https://doi.org/10.1038/nature06018

Hanson, L. G. (1970). *The origin and Development of Moses Coulee and other Scabland features on the Waterville Plateau, Washington* (p. 154). University of Washington, PhD Dissertation.

Harpel, C. J. (1996). *Paleodischarges and inferred hydraulics of the Missoula floods: Columbia River valley and Channeled Scabland, eastern Washington*. (Undergraduate Thesis) Western Washington University.

Harpel, C. J., Waitt, R. B., & O'Connor, J. E. (2000). Paleodischarges of the late Pleistocene Missoula floods, eastern Washington, USA (Abstract, Orkustofnun Rept. OS-2000/036). In *Extremes of the Extremes Conference* (p. 21).

Hoek, E., & Bray, J. (1981). *Rock Slope Engineering* (Rev. 3. ed.). Institution of Mining and Metallurgy.

Hoek, E., & Brown, E. T. (1997). Practical estimates of rock mass strength. *International Journal of Rock Mechanics and Mining Sciences*, *34*(8), 1165–1186. https://doi.org/10.1016/S1365-1609(97)80069-X

Hurst, A. A., Anderson, R. S., & Crimaldi, J. P. (2021). Toward entrainment thresholds in fluvial plucking. *Journal of Geophysical Research: Earth Surface*, *126*(5). https://doi.org/10.1029/2020JF005944

Kehew, A. E. (1982). Catastrophic flood hypothesis for the origin of the Souris spillway, Saskatchewan and North Dakota. *Geological Society of America Bulletin*, *93*(10), 1051–1058. https://doi.org/10.1130/0016-7606(1982)93<1051:CFHFTO>2.0.CO;2

Komatsu, G., & Baker, V. R. (1997). Paleohydrology and flood geomorphology of Ares Vallis. *Journal of Geophysical Research: Planets*, *102*(E2), 4151–4160. https://doi.org/10.1029/96JE02564

Komatsu, G., Miyamoto, H., Ito, K., Tosaka, H., & Tokunaga, T. (2000). The Channeled Scabland: Back to Bretz? Comment and Reply. *Geology*, *28*(6), 573–574. https://doi.org/10.1130/0091-7613(2000)28<573:TCSBTB>2.0.CO;2

Lamb, M. P., & Dietrich, W. E. (2009). The persistence of waterfalls in fractured rock. *Geological Society of America Bulletin*, *121*(7–8), 1123–1134. https://doi.org/10.1130/B26482.1

Lamb, M. P., Dietrich, W. E., Aciego, S. M., DePaolo, D. J., & Manga, M. (2008). Formation of Box Canyon, Idaho, by megaflood: Implications for seepage erosion on Earth and Mars. *Science*, *320*(5879), 1067–1070. https://doi.org/10.1126/science.1156630

Lamb, M. P., Finnegan, N. J., Scheingross, J. S., & Sklar, L. S. (2015). New insights into the mechanics of fluvial bedrock erosion through flume experiments and theory. *Geomorphology*, *244*, 33–55. https://doi.org/10.1016/j.geomorph.2015.03.003

Lamb, M. P., & Fonstad, M. A. (2010). Rapid formation of a modern bedrock canyon by a single flood event. *Nature Geoscience*, *3*(7), 477–481. https://doi.org/10.1038/ngeo894

Lamb, M. P., Mackey, B. H., & Farley, K. A. (2014). Amphitheater-headed canyons formed by megaflooding at Malad Gorge, Idaho. *Proceedings of the National Academy of Sciences*, *111*(1), 57–62. https://doi.org/10.1073/pnas.1312251111

Lang, K. A., Huntington, K. W., & Montgomery, D. R. (2013). Erosion of the Tsangpo Gorge by megafloods, Eastern Himalaya. *Geology*, *41*(9), 1003–1006. https://doi.org/10.1130/G34693.1

Lapotre, M. A., & Lamb, M. P. (2015). Hydraulics of floods upstream of horseshoe canyons and waterfalls. *Journal of Geophysical Research: Earth Surface*, *120*(7), 1227–1250. https://doi.org/10.1002/2014JF003412

Lapotre, M. G. A., Lamb, M. P., & Williams, R. M. E. (2016). Canyon formation constraints on the discharge of catastrophic outburst floods of Earth and Mars. *Journal of Geophysical Research: Planets*, *121*(7), 1232–1263. https://doi.org/10.1002/2016JE005061

Larsen, I. J., & Lamb, M. P. (2016). Progressive incision of the Channeled Scablands by outburst floods. *Nature*, *538*(7624), 229–232. https://doi.org/10.1038/nature19817

Larsen, I. J., & Montgomery, D. R. (2012). Landslide erosion coupled to tectonics and river incision. *Nature Geoscience*, *5*(7), 468–473. https://doi.org/10.1038/NGEO1479

Lewis, A. R., Marchant, D. R., Kowalewski, D. E., Baldwin, S. L., & Webb, L. E. (2006). The age and origin of the Labyrinth, western Dry Valleys, Antarctica: Evidence for extensive middle Miocene subglacial floods and freshwater discharge to the Southern Ocean. *Geology*, *34*(7), 513–516. https://doi.org/10.1130/G22145.1

Lorig, L., & Varona, P. (2001). Practical slope-stability analysis using finite-difference codes. In W. A. Hustrulid, M. J. McCarter, & D. J. A. Van Zyl (Eds.), *Slope stability in surface mining* (pp. 115–124). Society for Mining Metallurgy and Exploration.

Malde, H. E. (1968). The catastrophic late Pleistocene Bonneville flood in the Snake River Plain, Idaho. *U.S. Geological Survey Professional Paper*, *596*, 1–52. https://doi.org/10.3133/pp596

Manga, M. (2004). Martian floods at Cerberus Fossae can be produced by groundwater discharge. *Geophysical Research Letters*, *31*(2). https://doi.org/10.1029/2003GL018958

Miyamoto, H., Komatsu, G., Baker, V. R., Dohm, J. M., Ito, K., & Tosaka, H. (2007). Cataclysmic Scabland flooding: Insights from a simple depth-averaged numerical model. *Environmental Modelling & Software*, *22*(10), 1400–1408. https://doi.org/10.1016/j.envsoft.2006.07.006

Montgomery, D. R., Hallet, B., Yuping, L., Finnegan, N., Anders, A., Gillespie, A., & Greenberg, H. M. (2004). Evidence for Holocene megafloods down the Tsangpo River Gorge, southeastern Tibet. *Quaternary Research*, *62*(2), 201–207. https://doi.org/10.1016/j.yqres.2004.06.008

O'Connor, J. E. (1993). Hydrology, hydraulics and geomorphology of the Bonneville flood. *Geological Society of America Special Papers*, *274*(83). https://doi.org/10.1130/SPE274-p1

O'Connor, J. E., & Baker, V. R. (1992). Magnitudes and implications of peak discharges from glacial Lake Missoula. *Geological Society of America Bulletin*, *104*(3), 267–279. https://doi.org/10.1130/0016-7606(1992)104<0267:maiopd>2.3.co;2

O'Connor, J. E., Baker, V. R., Waitt, R. B., Smith, L. N., Cannon, C. M., George, D. L., & Denlinger, R. P. (2020). The Missoula and Bonneville floods—A review of ice-age megafloods in the Columbia River basin. *Earth-Science Reviews*, *208*, 103181. https://doi.org/10.1016/j.earscirev.2020.103181

Pardee, J. T. (1942). Unusual currents in Glacial Lake Missoula, Montana. *Geological Society of America Bulletin*, *53*(11), 1569–1600. https://doi.org/10.1130/GSAB-53-1569

Praetorius, S. K., Condron, A., Mix, A. C., Walczak, M. H., McKay, J. L., & Du, J. (2020). The role of Northeast Pacific meltwater events in deglacial climate change. *Science Advances*, *6*(9). https://doi.org/10.1126/sciadv.aay2915

Roberts, S., Nielsen, O., Gray, D., Sexton, J., & Davies, G. (2015). *ANUGA user manual Release 2.0*. https://doi.org/10.13140/RG.2.2.12401.99686

Schlichting, H. (1979). *Boundary-layer theory* (7th ed.) McGraw-Hill.

Schmeeckle, M. W., Nelson, J. M., & Shreve, R. L. (2007). Forces on stationary particles in near-bed turbulent flows. *Journal of Geophysical Research*, *112*(F2). https://doi.org/10.1029/2006JF000536

Schmidt, K. M., & Montgomery, D. R. (1995). Limits to relief. *Science*, *270*(5236), 617–620. https://doi.org/10.1126/science.270.5236.617

Schultz, R. A. (1995). Limits on strength and deformation properties of jointed basaltic rock masses. *Rock Mechanics and Rock Engineering*, *28*(1), 1–15. https://doi.org/10.1007/BF01024770

Scott, W. E., Pierce, K. L., Bradbury, J. P., & Forester, R. M. (1982). Revised Quaternary stratigraphy and chronology in the American Falls area, southeastern Idaho. In B. Bonnichsen & R. M. Breckenridge (Eds.), *Cenozoic Geology of Idaho: Idaho Bureau of Mines and Geology Bulletin* (Vol. 26, pp. 581–595).

Sharp, R. P., & Malin, M. C. (1975). Channels on Mars. *Geological Society of America Bulletin*, *86*(5), 593–609. https://doi.org/10.1130/0016-7606(1975)86<593:COM>2.0.CO;2

Smith, L. N. (2006). Stratigraphic evidence for multiple drainings of glacial Lake Missoula along the Clark Fork River, Montana, USA. *Quaternary Research*, *66*(2), 311–322. https://doi.org/10.1016/j.yqres.2006.05.009

Stein, O. R., & Julien, P. Y. (1993). Criterion delineating the mode of headcut migration. *Journal of Hydraulic Engineering*, *119*(1), 37–50. https://doi.org/10.1061/(ASCE)0733-9429(1993)119:1(37)

Turzewski, M. D., Huntington, K. W., & LeVeque, R. J. (2019). The Geomorphic impact of outburst floods: Integrating observations and numerical simulations of the 2000 Yigong Flood, Eastern Himalaya. *Journal of Geophysical Research: Earth Surface*, *124*(5), 1056–1079. https://doi.org/10.1029/2018JF004778

van der Bilt, W. G. M., Barr, I. D., Berben, S. M. P., Hennekam, R., Lane, T., Adamson, K., & Bakke, J. (2021). Late Holocene canyon-carving floods in northern Iceland were smaller than previously reported. *Communications Earth & Environment*, *2*(1). https://doi.org/10.1038/s43247-021-00152-4

Venditti, J. G., Rennie, C. D., Bomhof, J., Bradley, R. W., Little, M., & Church, M. (2014). Flow in bedrock canyons. *Nature*, *513*(7519), 534–537. https://doi.org/10.1038/nature13779

Waitt, R. B. (1980). About forty last-glacial Lake Missoula jökulhlaups through southern Washington. *The Journal of Geology*, *88*(6), 653–679. https://doi.org/10.1086/628553

Waitt, R. B. (1985). Case for periodic, colossal jökulhlaups from Pleistocene glacial Lake Missoula. *Geological Society of America Bulletin*, *96*(10), 1271–1286. https://doi.org/10.1130/0016-7606(1985)96<1271:cfpcjf>2.0.co;2

Waitt, R. B. (2016). Megafloods and Clovis cache at Wenatchee, Washington. *Quaternary Research*, *85*(3), 430–444. https://doi.org/10.1016/j.yqres.2016.02.007

Waitt, R. B. (2021). Roads less travelled by: Pleistocene piracy in Washington's Northwest Channeled Scabland. In R. B. Waitt, G. D. Thackray, & A. R. Gillespie (Eds.), *Untangling the Quaternary period—A legacy of Stephen C. Porter, Geological Society of America Special Paper* (Vol. 548). https://doi.org/10.1130/SPE548

Waitt, R. B., Atwater, B. F., Hanson, M. A., Lehnigk, K. E., Larsen, I. J., Bjornstad, B. N., & O'Connor, J. E. (2021). Upper Grand Coulee: New views of a Channeled Scabland megafloods enigma. In *Geological Society of America Field Guide, Trip* (Vol. 421). https://doi.org/10.1130/2021.0062(07)

Waitt, R. B., Denlinger, R. P., & O'Connor, J. E. (2009). Many monstrous Missoula floods down Channeled Scabland and Columbia valley. In J. E O'Connor, R. J. Dorsey, & I. P. Madin (Eds.), *Volcanoes to vineyards: Geologic field trips through the dynamic landscape of the Pacific Northwest*, *Geological Society of America Field Guide* (Vol. 15, pp. 775–844). Geological Society of America. https://doi.org/10.1130/2009.fld015(33)

Waitt, R. B., O'Connor, J. E., & Harpel, C. J. (2000). Varying routings of repeated colossal jökulhlaups through the Channeled Scabland of Washington, USA (Abstract, Orkustofnun Rept. OS-2000/036). In E*xtremes of the Extremes Conference* (Vol. 27).

Waitt, R. B., & Thorson, R. M. (1983). The Cordilleran ice sheet in Washington, Idaho, and Montana. In H. E. Wright & S. C. Porter (Eds.), *Late-Quaternary Environments of the United States: The Late Pleistocene* (pp. 53–70). University of Minnesota Press.

Warner, N. H., Gupta, S., Kim, J. R., Lin, S. Y., & Muller, J. P. (2010). Retreat of a giant cataract in a long-lived (3.7–2.6 Ga) Martian outflow channel. *Geology*, *38*(9), 791–794. https://doi.org/10.1130/G31268.1

Warner, N. H., Sowe, M., Gupta, S., Dumke, A., & Goddard, K. (2013). Fill and spill of giant lakes in the eastern Valles Marineris region of Mars. *Geology*, *41*(6), 675–678. https://doi.org/10.1130/G34172.1

Wilson, L., Ghatan, G. J., Head III, J. W., & Mitchell, K. L. (2004). Mars outflow channels: A reappraisal of the estimation of water flow velocities from water depths, regional slopes, and channel floor properties. *Journal of Geophysical Research*, *109*(E9). https://doi.org/10.1029/2004JE002281

Wyllie, D. C. (2017). Rock strength properties and their measurement. In *Rock slope engineering* (5th ed., pp. 117–162). CRC Press. https://doi.org/10.1201/9781315154039-6

Wyllie, D. C., & Mah, C. W. (2004). *Rock slope engineering: Civil and mining* (4th ed.). Taylor and Francis. https://doi.org/10.1201/9781315274980

Reference From the Supporting Information

Hanson, L. G., Kiver, E. P., Rigby, J. G., & Stradling, D. F. (1979). *Surficial geologic map of the Ritzville quad, Washington* (Open File Report 79-10 ed.). Washington Division of Geology and Earth Resources, scale 1:250,000.